Metallurgical report on samples from eight iron mining tools from Combe Down, Stone

Introduction

The artefacts samples consisted of seven quarrying wedges and one saw. These covered the periods from phase 1 to phase 6 of the underground quarrying, that is dating from the late17th century until 1935. This period covers the industrial revolution and hence a number of major technology changes in the means of production of iron and steel. The earliest iron production method was the bloomery or direct process in which iron was smelted directly from its ore to a solid mass of iron with a high slag content – the bloom. The resultant bloom then had to be forged further at high temperatures to remove as much of the slag as possible and the break up the slag remaining in the metals so that its effects were not excessively detrimental. This method of iron production was the principal method by which iron was produced in the West from the beginning of the Iron Age until the introduction of the blast furnace in the later medieval period. With the introduction of the blast furnace, or indirect process, the primary product of the smelting process was cast iron that is iron with sufficiently high carbon content so that it could be tapped out of the furnace as liquid metal. In Europe the process appear to have started developing commercially around the Liège region around 1300, although there is evidence of the process having been used earlier in Sweden. In Britain the blast furnace arrived in the Wealden region in the 1490s (Cleere and Crossley, 111-121), where it was primary used for the production of ordinance. However, at times when the military demand on these furnaces was low they would produce cast domestic ware and ingots of pig iron to be converted into malleable bar iron. The pig iron was fed into oxidizing part refining hearth so that carbon in the cast iron would be burnt out. As this happened the melting temperature of the metal would rise, until a ball of pasty iron and slag formed which would be forged out into bars of wrought iron.

The blast furnaces and associated forges were initially situated in places like the Weald where there was both iron ore and a suitable large supply of fuel in the form of wood, which could be to be converted to charcoal to feed both the blast furnaces and finery forges. By the end of the seventeenth century the indirect (blast furnace) smelting of iron had largely replaced the bloomery process over the southern part of the British Isles, although the bloomery process lingered on in the 18th century in North West of England, and was still used extensively in more advanced forms during the 19th century in parts of Europe and the United States of America.

By the early eighteen century there was considerable economic pressure on the woodland resources around London, and hence pressure to move the iron industries regions where the economic conditions were more suitable – woodlands were cheaper and there good means of transport, hence

there was an expansion of the industry in Shropshire, the Forest of Dean and South Wales. Also, there was still a continued pressure to use mineral coal rather than charcoal as fuel for the smelting process and the subsequent fining processes. The problem associated with the use of coal was that most coal contains sulphur, and is reduced during smelting and is dissolved in cast iron. This it is not much of a problem as long as there is sufficient manganese present to mop up the sulphur as MnS. The sulphur from the use of coal in the conversion of cast iron into wrought iron would it makes the metal 'hot short', that is brittle the metal at high temperatures. This problem was initially solved by Abraham Derby at the Coalbrookdale Furnace, Iron Bridge in 1709. Where the local coal is both suitable to make reactive coke and has low sulphur content. However this was not the situation throughout the country, it was some time before smelting with coal converted to coke became widely accepted. The other problem with main British iron ores is that they have a relatively high phosphorus content. This has two effects; it inhibits the diffusion of carbon into the iron during the conversion of wrought iron to steel; secondly it makes the wrought iron work-harden rapidly. Although not all British iron ores have a high phosphorus content, as the early steel makers did not understand the nature of the problem they in general think that British iron to be acceptable for the production of steel. The steel producers preferred to use trusted imported iron from the Baltic or Spain. The other effect of phosphorus was to make the metal cold-short, which is the rapid work-hardening when the metal was forged at low temperature. As wrought iron was normally worked at red heat for forging operations, or white heat for welding, this was not a problem for many artefacts. It may have been that the possibility of improving the mechanical properties of high phosphorus iron have been utilized since the Iron Age (Ehrenreich 1985, 82), and in the 19th century (wire ?) nail-makers preferred to use high phosphorus metal.

Although Tylecote (1976, 107) states that until about 1770 the charcoal-fire finery was the only satisfactory way of converting pig iron to malleable iron. This technique did have the disadvantage that it could not remove any sulphur from the metal. However during the 18th century there were a number of experiments with methods of refining cast iron to wrought iron using coal fired fineries to carry out a two stage conversion process. The second stage of the process was being to 'pot and stamp' the metal. That is the broken up fined metal was put in clay pots with kelp and other alkali fluxes and heated in a coal-fired reverberatory furnace. The alkalis present would help to reduce the sulphur content of the metal. There has been discussion as to the history of the introduction of the true puddling process, in which the refining of cast iron is carried out directly in the bed of a reverberatory furnace. Day and Tylecote (1991, 236) admit that the Crannage brothers fined cast in a air furnace (reverberatory), but they don't think that process was in fact used. However, Hayman (2004, 116) quotes an account of 1768 describing what can only be puddling carried out at the Coalbrookdale Upper Forge using a mixture of pig and scrap iron. And suggest that it was forged into flat bars for tyres and for rolling into plate. However, it use at Coalbrookdale was limited due to the high wastage of metal in the conversion process and the inconsistent quality of the metal produced. The puddling process only came into its own when Henry Cort combined the idea of puddling as used by the Crannage brothers with the use of grooved rolls to work the iron extensively (1784 patent). This got round the inconsistent quality of the iron that had been produced at Coalbrookdale (Hayman 2004, 118).

Over the period from 1818 to 1830s the dry puddling process as patented by Cort was improved by first Rogers and then Hall. The sand base of the Cort puddling hearth was replaced partially by iron oxide in the form of iron-rich cinder and slag. This resultant reaction between the carbon in the cast iron and the oxygen in the iron oxide resulted in the production of carbon monoxide bubbling through the slag bath. This version of the process came to be known as wet puddling. There were further

important developments in the latter half of the 19th century (the Bessemer process 1856, the Siemens-Martin open hearth 1865, Bessemer-Thomas process 1879). These convertors ran at temperatures above the melting point of the metal so they produced mild steel rather than hot but solid wrought iron.

Methodology

Sampling and Preparation

Sample preparation.

The samples were cut from the blade section of the wedges using a V-shaped cut to obtain a section that was between 15mm and 20 mm long. The sections were then mounted in cold-setting epoxy resin and polished as for a standard metallographic examination. That is ground using silicon carbide papers grade 120 through to 1200 and then diamond polished to a 1 micron finish. In the case, of these samples it proved particularly difficult to get a good final polish due to presence of a high density of slag inclusions which were often fractured and fell out scratching the polished surface. Once polished the samples were carbon coated for examination in the electron-probe micro-analyser (EPMA) to determine the composition of the metal and in the scanning electron microscope to examine the slag inclusions. After the analysis of the metal and the slag inclusions, the carbon coat was removed by a further one micron polish. The samples were then etched in 2% nital to reveal the microstructure, and finally the samples were subjected to micro-hardness testing.

Analytical

Metal

The composition of the metal was measured separately from that of the slag inclusions. The measurements were carried out using a JEOL 8800 electron micro-probe analyser (EPMA) putting the electron beam down on a number of spots and detecting the X-rays generated. In addition, the samples were mapped for the elements Si,Ni, The same the elements aluminium, silicon, phosphorus, sulphur, titanium, vanadium, chromium, manganese, cobalt, nickel, zinc, arsenic and molybdenum were analyzed in all the samples. In most samples aluminium, silicon, titanium, vanadium, chromium, manganese, zinc and molybdenum were not detected at concentrations above their detection limits. For most of these elements this is not surprising, as if they were originally present in the cast iron they would have been burnt out of the metal during the fining process.

Slag inclusions

There were problem with the retention of the slag inclusions as they appear to have been worked below their glass transition temperature and had in places extensively fractured. This could have been due to the cold work of the metal during use of the tools, however, there were no signs of gross mechanical deformation of the iron grains except close to the surface. The inclusions were analysed

using the ‘Feature’ method of an Oxford Instruments INCA Energy Dispersive Detector system on a JEOL 6480LV Scanning Electron Microscope (SEM). In the past such analysis was time consuming as it required a extensive human intervention of find ‘representative’ inclusions and aim the electron beam and acquire the X-ray data. However, the slag inclusions in wrought tend to be heterogeneous, therefore, Rostoker and Dvorak (1990, 164) suggested that any analysis of the slag inclusions should analyse at least 10 inclusions. However, the time and cost of such as analysis restricted Mackenzie and Whiteman (2006, 143) to as few as 8 inclusions in each sample. With the use of digital image capture of the back-scattered electron image, accurate computer controlled microscope stages, improved X-ray detectors and detector geometries it is now possible to automate the process so that several hundred or thousand inclusions can be analysed in automated overnight runs. The problem has now become that of finding a suitable method of analyzing and presenting the data acquired and relating that to the metallurgy involved. As well as determining the chemistry of the inclusions, the same method was used to determine the number, size, and area fraction of the slag inclusions in the samples.

The hardness which gives an indication of the mechanical properties of the metal was determined using a W and W Vickers microhardness tester. For each sample a series of test points separated by approximately 0.5 mm was carried out at a distance of 5 mm from the point where the sample was detached from the object. It was noticeable that the hardness of many of the wedges increased close to the surface without any obvious increase int he carbon content.

Once etched, the samples were examined using a Polyvar optical microscope fitting with the Leica Materials-Workstation software to determine the grain-size. The hardness results are presented in terms of the ASTM grain size number **G** according to the equation -

$$n = 2^{G-1}$$

Where **n** is the number of grain per square inch when the sample is magnified by 100 times. Thus the larger the grain size number the smaller the actual grain-size. The values presented in Table 1 are the average values, the compositional inhomogeneous nature of wrought iron and early steel is also reflected in the grain size.

Overall Results

The averaged data for all, obtained by the above analyses are presented below in tables 1 to 4. As most of the samples were of wrought iron, and or an inhomogeneous nature, within a sample values measured could vary considerably. The mean slag inclusion composition should not be considered as an accurate analysis of the inclusions due to a large number of complicating factors which will only be resolved by further research in this novel method of data gathering. One of the main problems was that the sizes of many of the inclusions were too small to stop the electron beam completely and as a result the compositions are likely to be high in iron. It would be possible to filter the result s in the database in terms of their physical dimensions and exclude any below a certain size limits but work to optimize these parameters is yet to be carried out. Therefore, for this project the data from all the slag inclusions found in the scanned area were included in the database. Normally, slag compositions would be given in terms of the oxides of the elements; however, in this case as one of the samples (sf 932) had a high proportion of iron/manganese inclusions the results are mean inclusion compositions are presented in Table 4 in terms of the element weight percent.

The metallography proved that all the wedges were essentially wrought iron that is iron with low carbon content. The one exception was the possible frig-bob saw (SF932) which was a relatively high carbon steel. The carbon content of this sample was hypereutectoid (above around 0.8 % C), whereas in the rest of the samples the carbon varied from zero to 0.25-0.3 % C. The presence of phosphorus was noticeably present in some of the samples as was shown by the presence of phosphorus 'ghosting' when viewing the samples under the metallurgical microscope.

Table Table of artefact samples and some metallurgical data

Sample	Tool	Phase	Period	Hardness	Hardness Std Dev	Grain Size	inclus % Area
632	Possible frig-bob saw	1	late 17th-early 18th C	261.4	24.7	12.8	0.03
917	wedge Type 1	1	late 17th-early 18th C	164.1	13.2	7.0	0.96
851	wedge Type 2	2	1729-1768	138.3	27.3	7.6	0.41
333	wedge Type 1	3 or 4	1768-1833	194.1	14.2	5.2	1.27
530	wedge Type 3	3 or 4	1768-1833	247.0	23.9	6.8	3.14
373	wedge Type 3	4	1800-1833	192.9	34.3	7.1	3.10
623	wedge Type 2	4 or 5	1800-1867	149.1	13.8	4.0	4.05
1030	wedge Type 2	6	1867-1935	214.9	24.2	7.3	3.55

Table Average metal composition determine by EPMA

Sample	Si	P	S	Co	Ni	Cu	As
632	0.096	0.040	0.010	0.032	0.003	0.208	0.006
917	nd	0.031	0.007	0.003	0.004	0.004	0.037
851	nd	0.117	0.006	0.002	0.003	0.011	0.007
333	nd	0.051	0.001	0.027	0.084	0.046	0.008
530	nd	0.128	0.005	0.014	0.031	0.048	0.005
373	nd	0.127	0.003	0.016	0.025	0.03	0.012
623	nd	0.071	0.003	0.015	0.024	0.014	0.001
1030	nd	0.147	0.002	0.015	0.022	0.03	0.017

nd = Not detected in any point

Table Mean slag inclusion dimensions for the various samples

Sample	Tool	Phase	No. of inclusions per mm^2	Mean Area In μm^2	Mean breath in µm.	Mean Length in µm.
632	Possible frig-bob saw	1	246	1.5	0.69	1.5
917	wedge Type 1	1	80	119.7	5.02	27.4
851	wedge Type 2	2	98	41.4	3.52	11
333	wedge Type 1	3 or 4	264	48	3.1	15.25
530	wedge Type 3	3 or 4	476	66	4	13.4
373	wedge Type 3	4	437	71	3.9	17.8
623	wedge Type 2	4 or 5	303	75	4.4	17.5
1030	wedge Type 2	6	517	68.6	3.71	18.3

Table Approximate Mean slag inclusion compositions in terms of elements weight percent.

Sample	632	917	851	333	530	373	623	1030
Phase	1	1	2	3 or 4	3 or 4	4	4 or 5	6
Na	0.15	0.22	0.21	0.26	0.16	0.11	0.11	0.13
Mg	0.21	0.74	0.63	0.28	0.12	0.13	0.08	0.24
Al	1.80	1.67	1.53	1.07	0.52	0.58	0.41	0.68
Si	7.88	4.74	5.92	6.85	4.84	2.79	2.28	7.85
P	0.18	1.55	2.43	2.39	5.01	4.48	3.74	4.59
S	5.40	0.60	0.37	0.26	0.71	0.39	0.61	0.39
K	0.24	0.71	0.85	0.41	0.14	0.10	0.07	0.13
Ca	1.21	1.23	4.22	0.88	0.50	1.59	0.11	0.46
Ti	0.90	0.11	0.13	0.11	0.11	0.08	0.10	0.20
Mn	6.58	0.18	0.32	0.88	1.03	0.39	0.65	2.21
Fe	66.97	73.52	66.83	70.67	70.44	68.71	77.09	63.84

Results

Saw (sf 632)

A tooth was sawn from the saw and sectioned in direction perpendicular to the plane of the saw blade. As Table 1 indicated this sample had a very fine microstructure, it was initially very difficult to determine the grain size, as it was to distinguish the grains from the fine duplex structure (Figure 1).

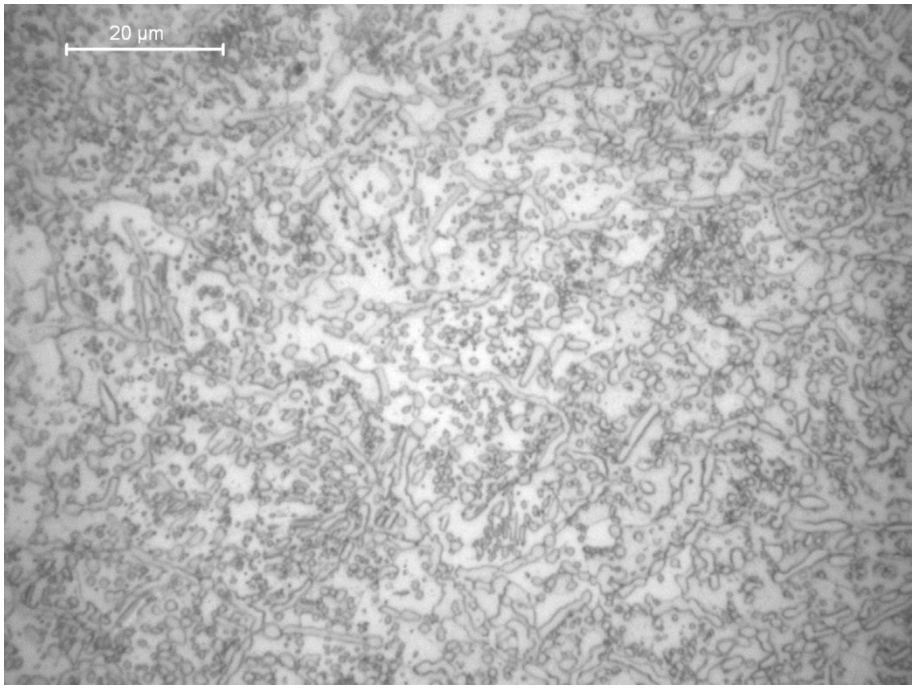

Figure . High magnification image of Section of the sf632 showing a duplex structure of primary cementite at the grain boundaries and in a matrix of ferrite within the grains.

At a lower magnification the sample showed distinct fine banding (Figure 2) but the structure still had a high carbon throughout all the bands. The high cementite (Fe3C) content of this sample shows that this was a hypereutectoid plain carbon steel. The small grain size and fine banding would suggest the steel had been forged down from an inhomogeneous bar. The microstructure would not suggest that there had been any attempt to quench and temper the saw blade, rather that it had been cooled a moderate rate so that there some evidence of mild spheroidization of the cementite. The hardness and the microstructure are what might be expected of a steel of this composition and would be suitable for a rock-saw, although it would have been possible to improve the mechanical properties by heat treatment this does not appear to have been done. The area fraction of slag inclusions in this sample was very low (Table 1), and this was the only sample in which silicon was detected in the metal. The phosphorus content was low which would have been helpful for the conversion of wrought iron into steel. This was the only sample with a high copper content

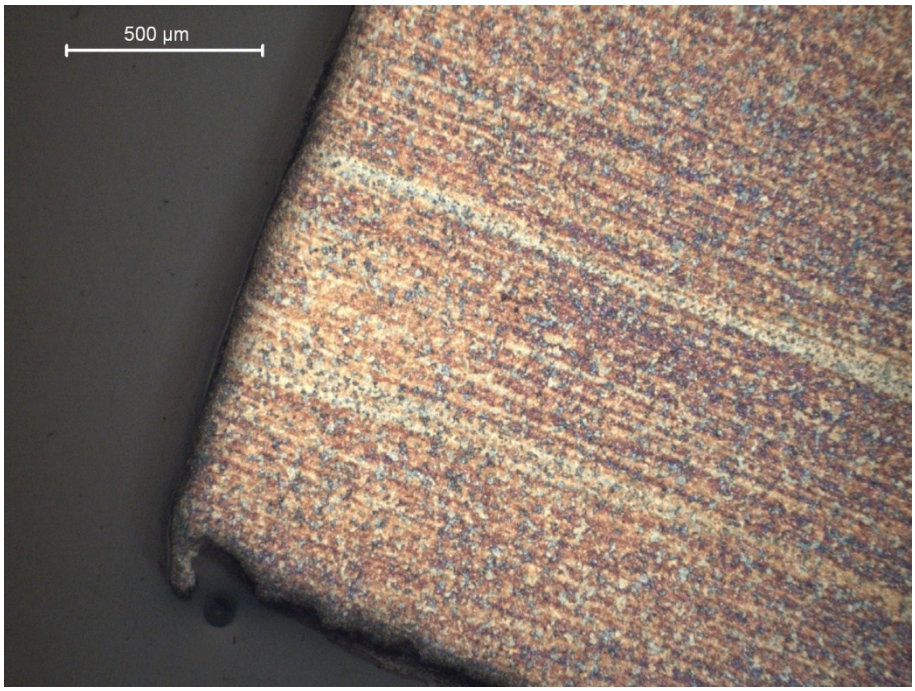

Figure Low magnification image of section of saw tooth showing the fine banding parallel to the plane of the saw blade

One possible interpretation of the structure that this high carbon steel (with carbon content between 1 and 1.3wt carbon) was a shear steel. Shear steel was produced by piling and forging blister steel. Blister steel was produced by heating bars of wrought iron in large sealed stone boxes with carburizing agents in a cementation furnace for up to nine days. During the carburization process the iron oxide in the slag inclusions was reduced to metallic iron generating voids. However, Mackenizie and Whiteman, 2006, 148, state that thermodynamic calculations show that elements such as Mn, Si, Al, and Ca cannot be significantly reduced in a cementation furnace. However, with this sample there was a significant amount of silicon present in the metal which is consistent with puddle iron.

The slag inclusions of this sample were odd in that of the 1290 inclusions examined over 17% had sulphur contents over 10 wt %. Figures 3 and 4 show the spectra from two of these inclusions that have high sulphur and manganese contents.

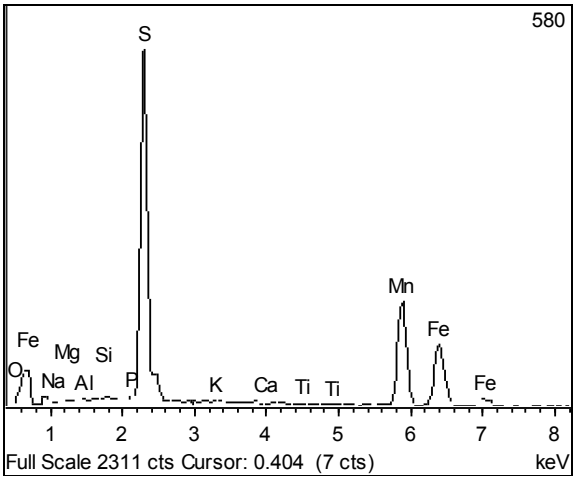

Figure Spectra from slag Inclusions from sample 632 showing high manganese content

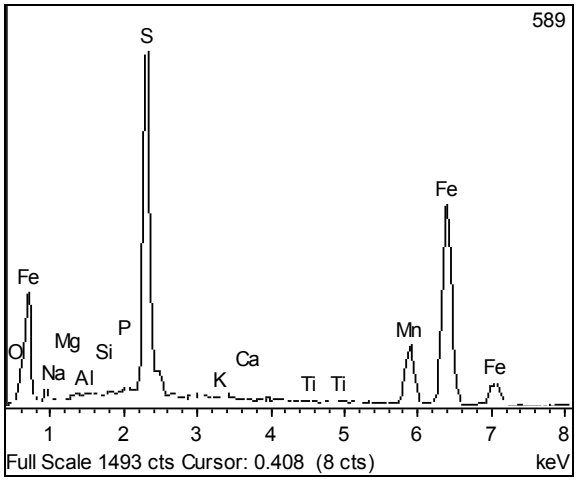

Figure Sulphide slag inclusion showing an excess of iron.

The spectra shown in Fig 4 might suggest that there was insufficient manganese present to make sure that all the sulphur was combined as MnS, if this was the case then deleterious FeS might start to form making the steel brittle at high temperatures. In addition to these sulphide inclusions, another less common class sulphide inclusion is illustrated in Fig 5.

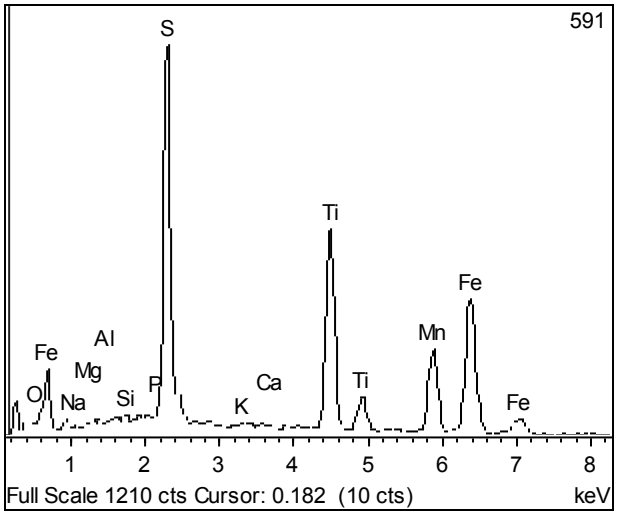

Figure A titanium containing sulphide inclusion from sample 632.

Although the exact composition of these inclusions is a little uncertain, as almost all the inclusion in this sample the inclusions are small, with a mean size of a little above one square micron which will result in some inaccuracy in the X-ray correction calculations. However, there can be no doubt about the presence of a large number of sulphur containing inclusions. This might suggest that coal was used at some stage in the production of this steel. In turn would suggest that this artefact dates to a period later than suggested by the archaeological phasing. The other types of inclusions observed were much as one might expect with simple single phase iron silicate inclusions making up 31% of the total number of analysed inclusions, and a variety of mixed sulphide and silicate inclusions contain significant amount of elements such as magnesium, aluminium, potassium and calcium. If this is shear steel formed from blister steel then it appears to have a much lower inclusion density

than the blister steel examined by Mackenizie and Whiteman, 2006 or by Rostoker and Dvorak (1988). The values would be much more like that one would expect from a liquid metal process such as crucible steel in which blister steel was melted in crucibles, however, it would seem unlikely that expensive crucible steel would be used make a relatively lowly artisan's tool.

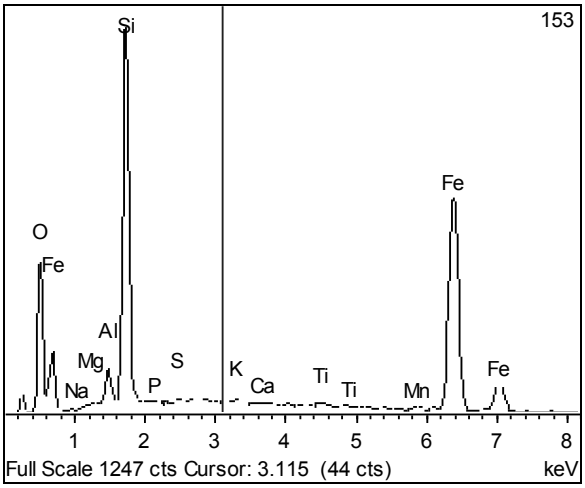

Figure Iron silicate inclusion

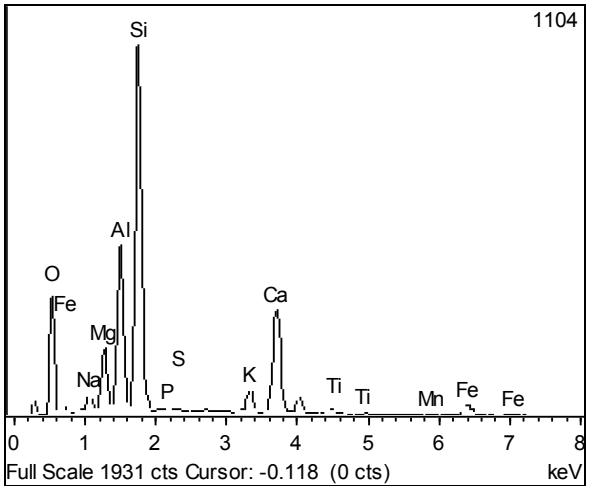

Figure Complex iron silicate inclusion

Of the remaining inclusions most of those that could be securely identified belong to the types illustrated in figures 6 and 7. That is either plain iron silicate inclusions or more complex inclusions often with less iron and more of the alkali elements. The hardness plot shows a relatively uniform and high profile.

Figure Plot of hardness against distance across sample.

SF917 (Wedge type 1)

The back-scattered electron image of this sample (Figure 9) and elemental maps (Figure 10) show two distinct regions in this sample.

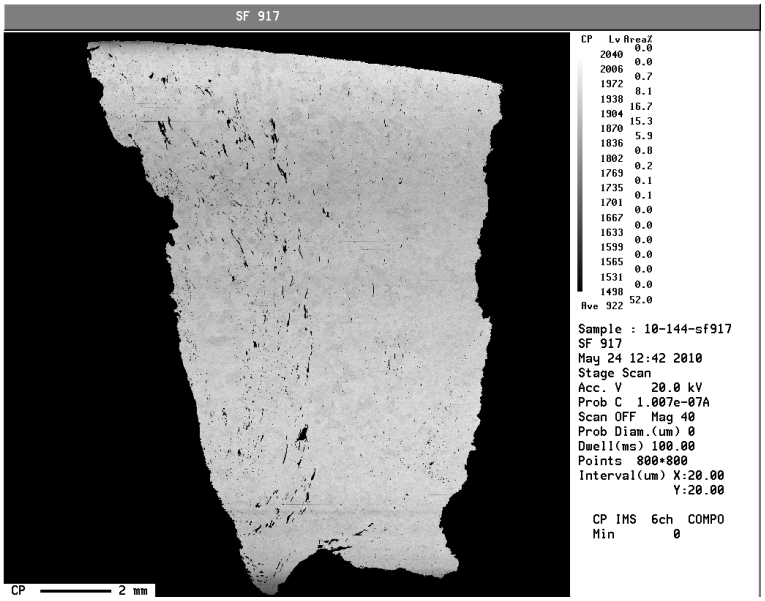

Figure Back-scattered electron image of Sample 917.

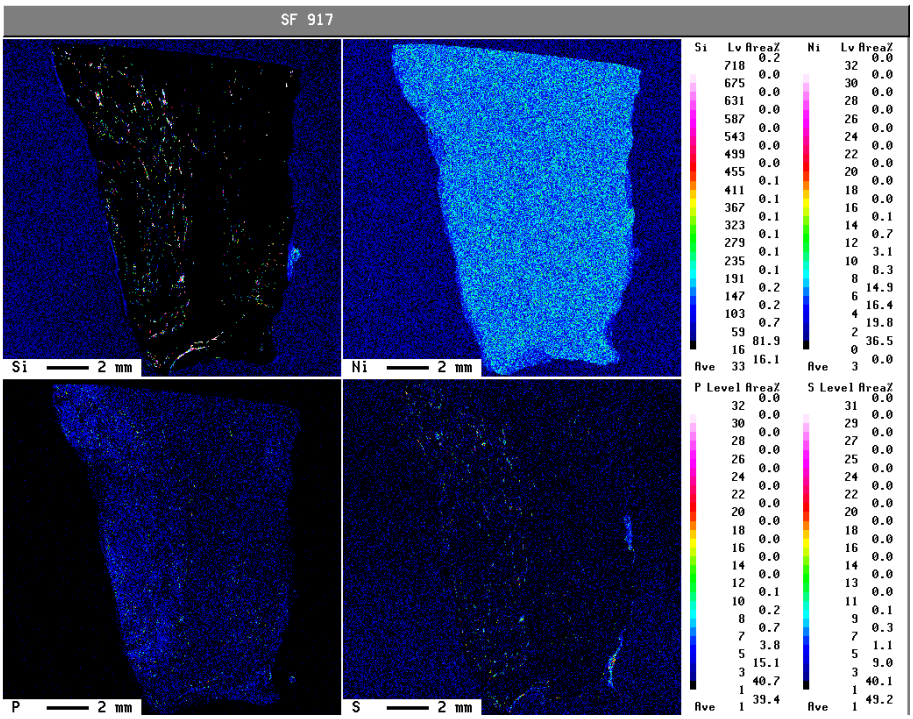

Figure Elemental maps from sample 917

A semi-circular patch to the left with a high inclusion density and enhanced levels of phosphorus (0.07 to 0.05 wt %) compared to the bulk of the material to the right which has both less inclusions and phosphorus (0.01-0.02 wt %). However, there was no obvious sign of a weld-line between the two regions. The metal in the higher phosphorus region showed a in the main consisted of areas large grains with interspersed regions with much smaller grain size (Figure 11).

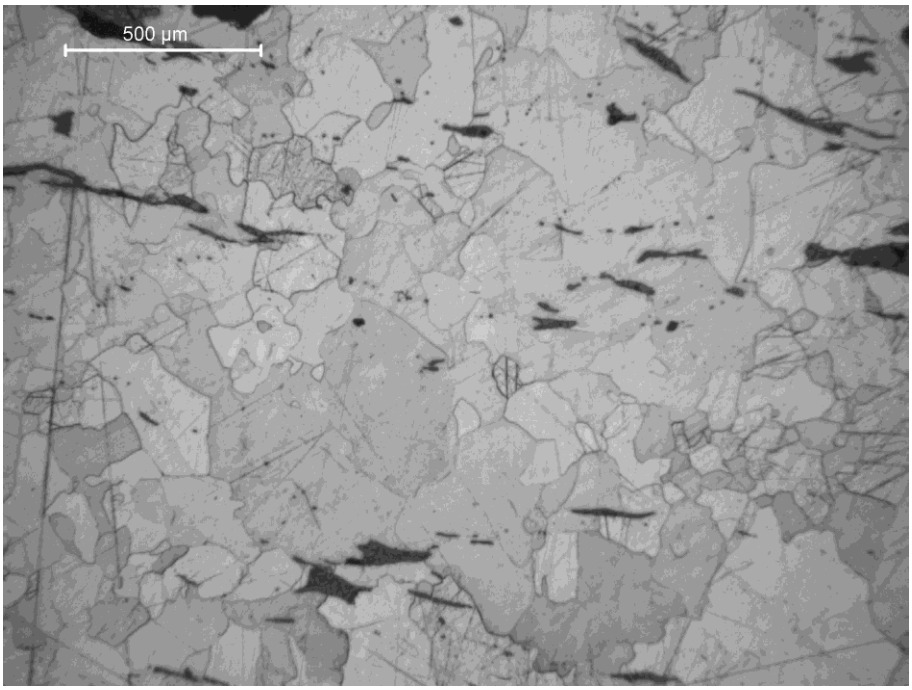

Figure Metallographic section of the high phosphorus region of Sample 917

The larger slag inclusions, which occurred predominantly in the high phosphorus part of the sample, tended to be two phase inclusions (Figure 12). The phases present were iron oxide (spectrum 1 Figure 12, illustrated Figure 13) growing in a globular or dendritic manner associated with the iron oxide wustite (FeO). The matrix was probably a glass as it contained in addition to iron and silicon it contained aluminium, potassium, calcium and appreciable amounts of phosphorus and sulphur (Figure 14). In all about 3000slag inclusions were analysis which when a ternary plot of their silicon, aluminium and calcium contents was generated showed two distinct groups (Figure 15). Initial analysis suggests that this separation may be due to the presence of two different types of inclusions within the two areas. The larger two phase inclusions seen in Figure 12 associated with the high phosphorus region, and smaller single phase inclusions as illustrated by the image and spectrum of Figure 16. However, the position is more complex as a ternary plot of aluminium, calcium and magnesium shows the separation of a group of inclusions rich in magnesium and calcium. Although the glass phase of the two phase inclusions could at times contain relatively high levels of sulphur (Figure 14), the overall average appears to be similar to most of the other samples with the exception of the saw (sf 632). In most of these inclusions the sulphur appears to be entirely combined within the glassy phase as no iron or iron/manganese sulphide was observed. However, there were a few inclusions where there was only iron, oxygen and sulphur present, suggesting the presence of iron sulphide. This was one of the two samples where the potassium content of the slag inclusions was relatively high. It is clear that further study of the chemistry, morphology and distribution of the slag inclusions would help in the understanding of the slag formation processes involved during the manufacture of wrought iron.

The hardness showed an increase toward the surface, but also there was an increase of hardness, as might be expected in the high phosphorus regions, in a wrought iron with carbon content no higher than 0.15%.

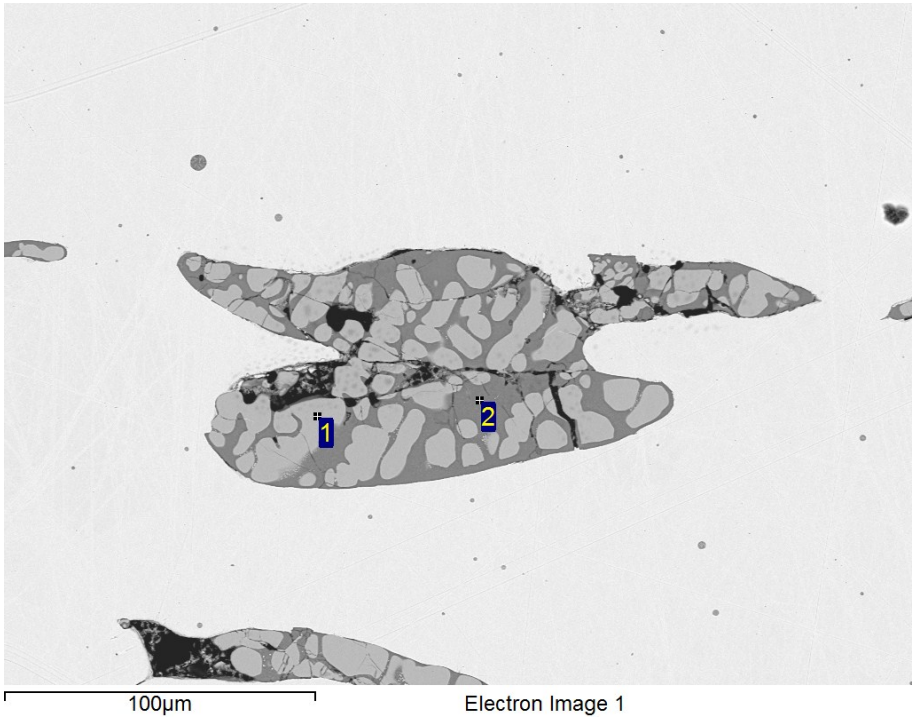

Figure Two phase slag inclusion in the high phosphorus region

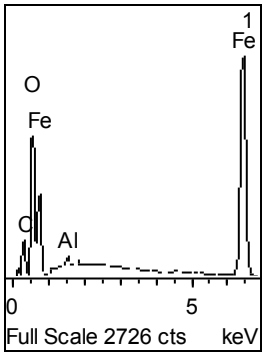

Figure Iron oxide phase

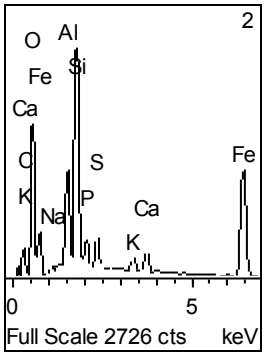

Figure 'Glass' matrix

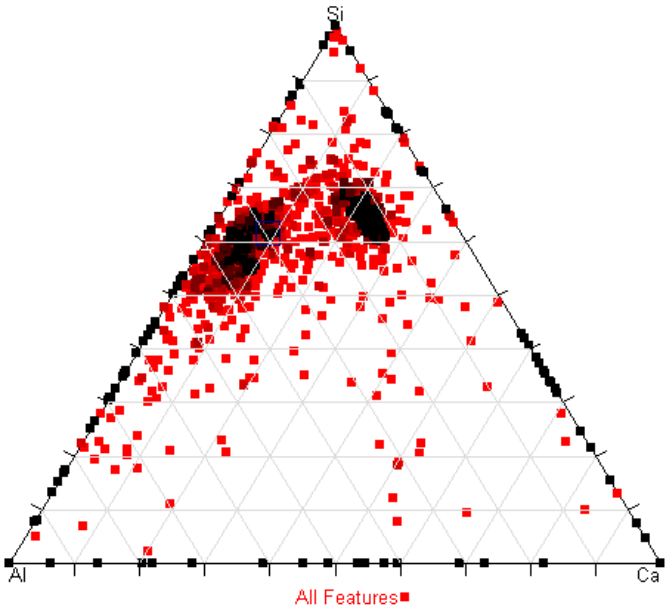

Figure Plot of silicon, aluminium and calcium as a ternary diagram. Each point represents the composition of one inclusion.

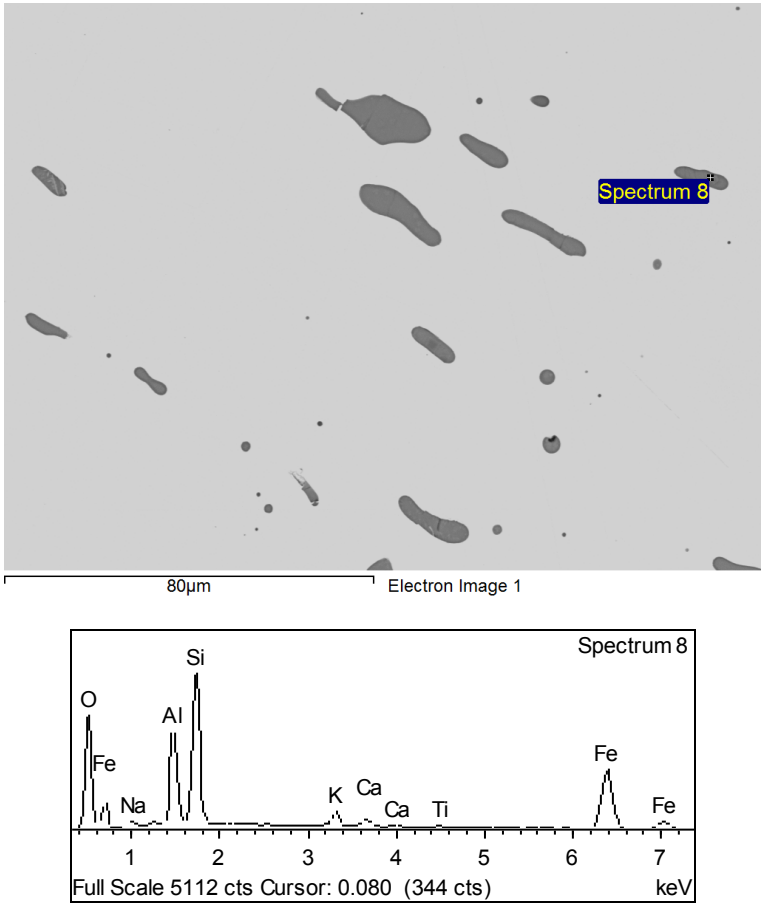

Figure Small single phase inclusions and spectrum associated with lower phosphorus region.

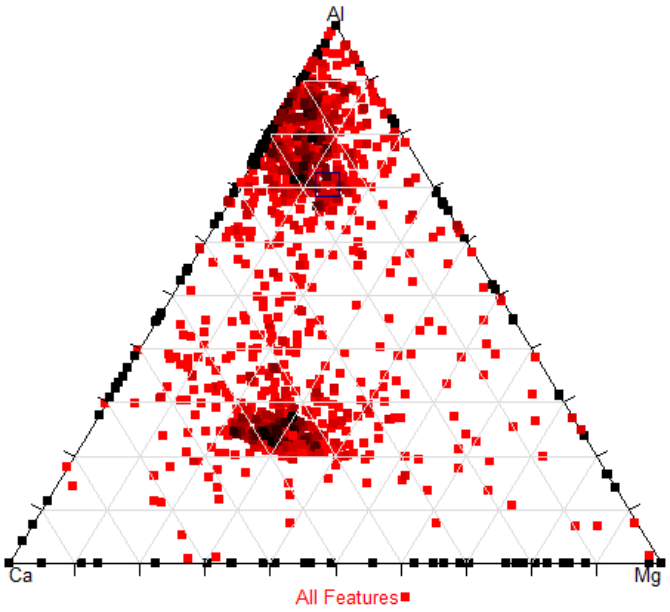

Figure Ternary plot of aluminium, calcium and magnesium.

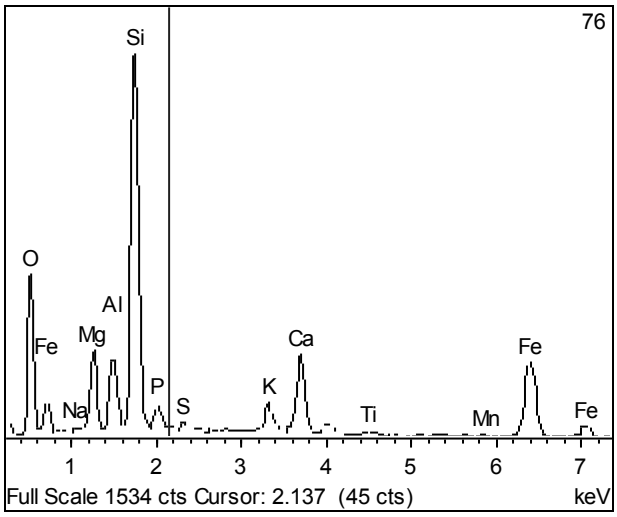

Figure Spectrum from one of the inclusions from the higher Ca-Mg group

Figure Plot of hardness against distance across sample (direction reverse of Figures 9 and 10)

SF851 (Wedge type 2)

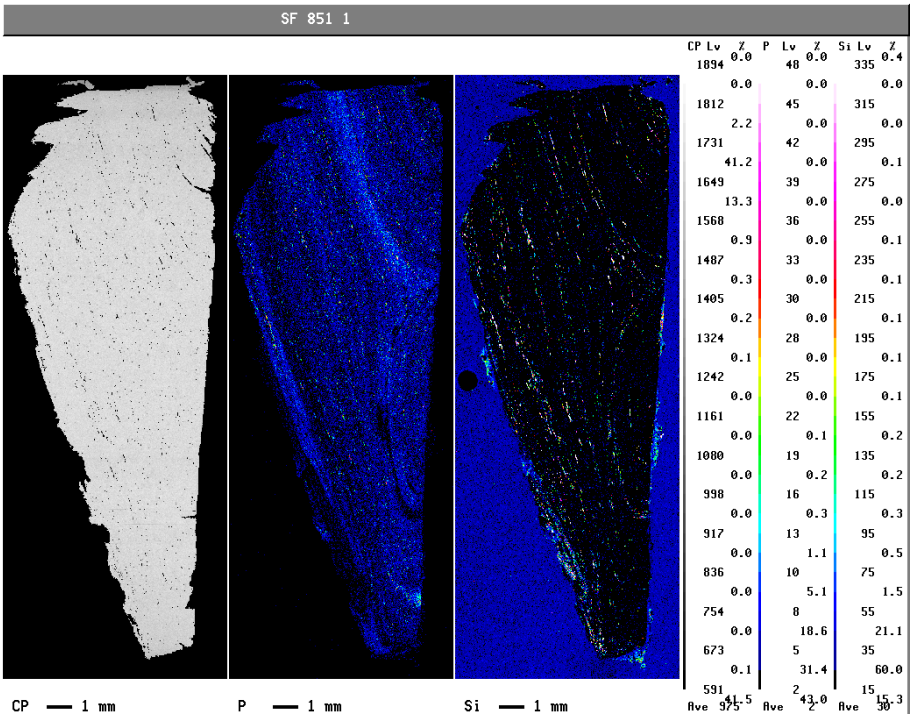

Figure Back-scattered electron image and phosphorus and silicon maps for sample SF851

The phosphorus and silicon maps show to that instead of the bands running down to the blade of the wedge the pattern is more complex. Both the phosphorus and the silicon bands on the right of the sample loop to the edge approximately a third of the way down. Where band with a high concentration of silicon (inclusions) and low phosphorus loops from the edge back towards the centre and then returns to edge with the width of the low phosphorus band increasing as it approached the cutting edge. This could well represent a weld-line in which metal dephosphorized during the process as well as local increasing the density of slag inclusions. However, in general the slag inclusions are relatively small and well broken up as illustrated by Figures 21 and 22. There was a variety of inclusion microstructures observed. The commonest being either the single phase or the two inclusions illustrated in Figure 23. The phase in the two phase inclusions were iron oxide (Fig 24) and a matrix with a composition similar to that seen in Figure 25. A third type of inclusion was identified in which there were three phases present (Figure 26). The phase were, small amounts of iron oxide with traces of vanadium, a small of 'glass', and the majority of the inclusion an iron silicate with minor amounts of calcium and magnesium present. The iron silicate was most likely to be of the olivine type (Fe_2SiO_4) given the analytical composition which was closer to an olivine composition than a pyroxene and the presence of free iron oxide. A ternary plot of silicon, calcium, and iron (Figure 27) showed the presence of two trend lines. The major one included the majority of the inclusions, and was a reflection of the relative proportion of iron oxide present. However, there was a second, less well defined, trend line with higher calcium to silicon ratio than the main line. On investigation the composition of these inclusions was high in phosphorus as well as calcium; however, they were not located within any specific area of the sample. This mean they were not directly related to the dephosphorized strip.

There were no inclusions with high sulphur contents.

The hardness of sample is surprising low given the structure and the phosphorus content; however, it does have the second largest grain size.

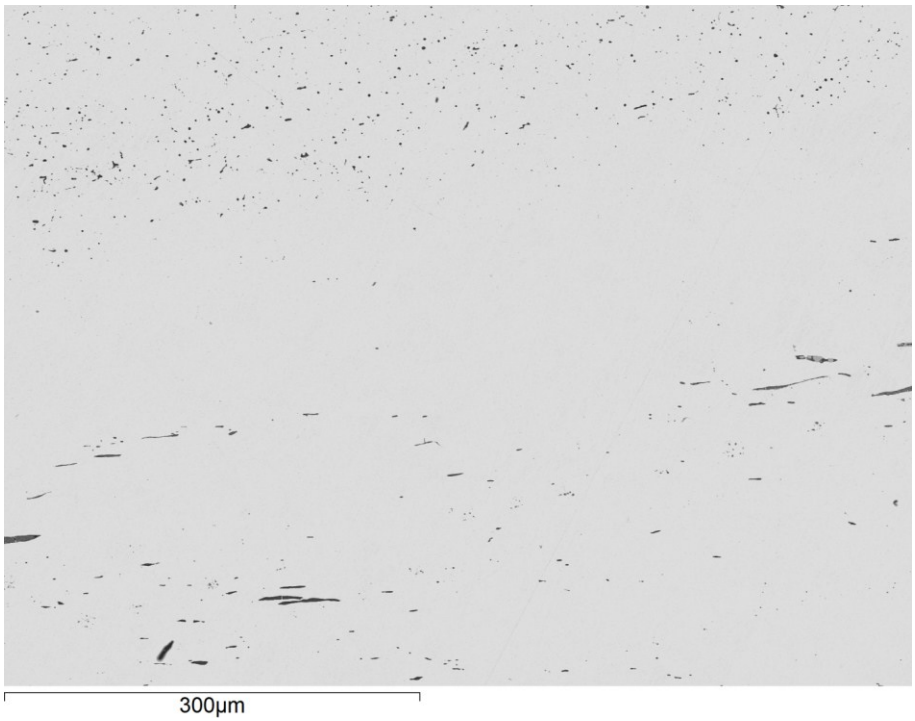

Figure Back-scattered Electron Image showing banded distribution of relatively small inclusions.

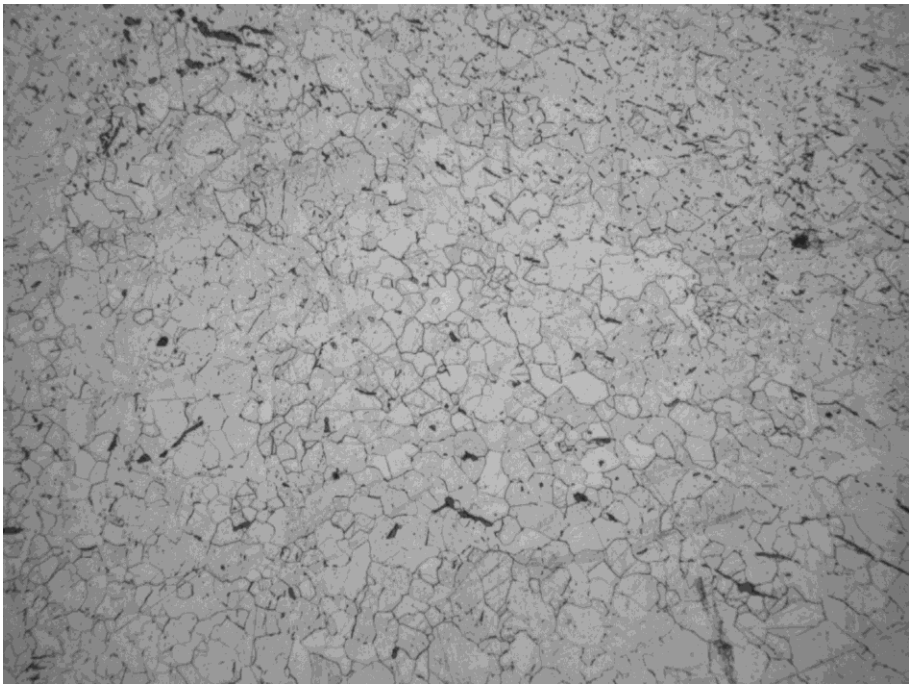

Figure Microstructure of comparative uniform sized grains but also local high density of small slag inclusions

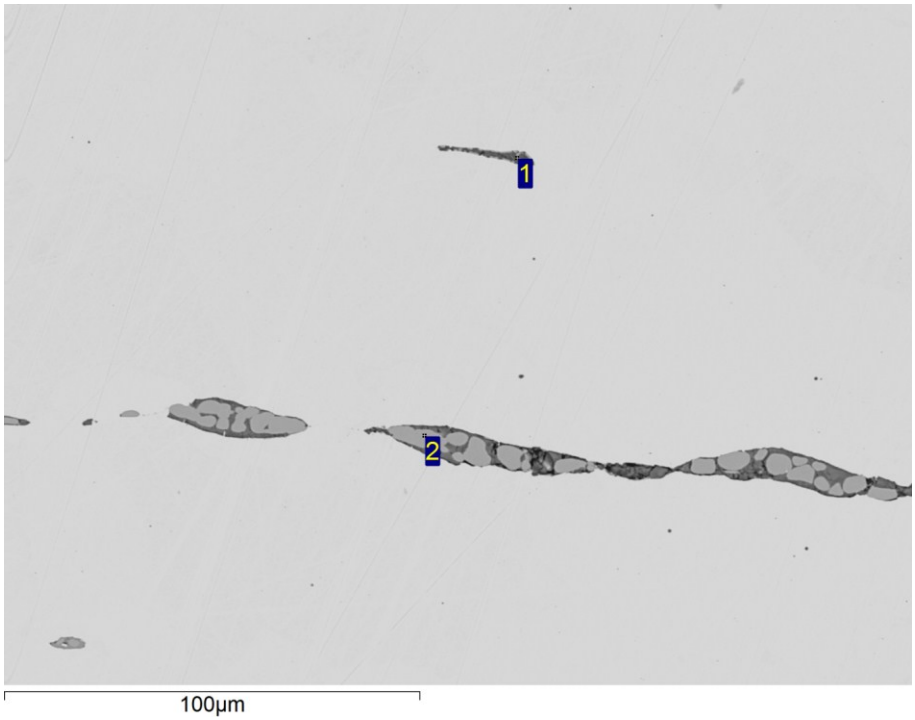

Figure Single phase (1) and two phase slag inclusions (2)

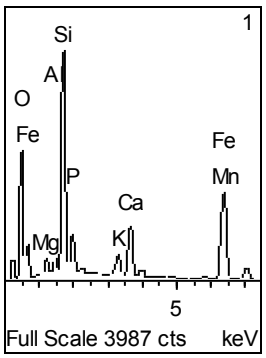

Figure Spectrum from single phase inclusion

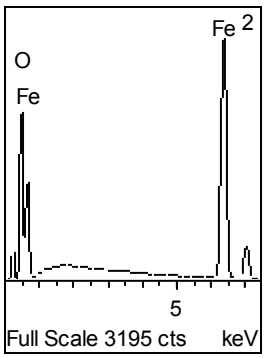

Figure Spectrum from bright phase in two phase inclusion

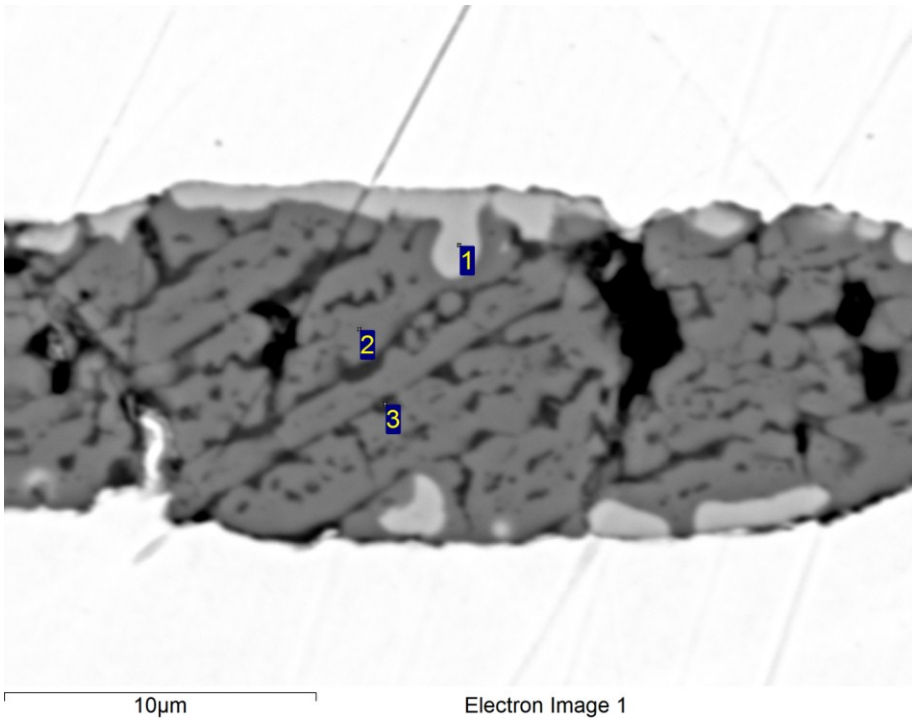

Figure Multi-phase inclusion composed of iron oxide (1), iron-silicate (2), and a 'glass' matrix (3) spectra are given below.

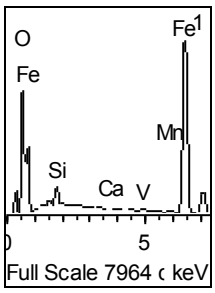

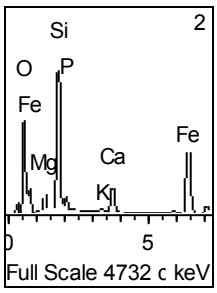

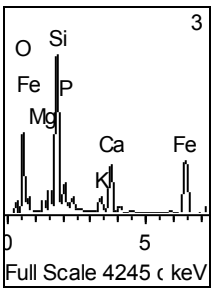

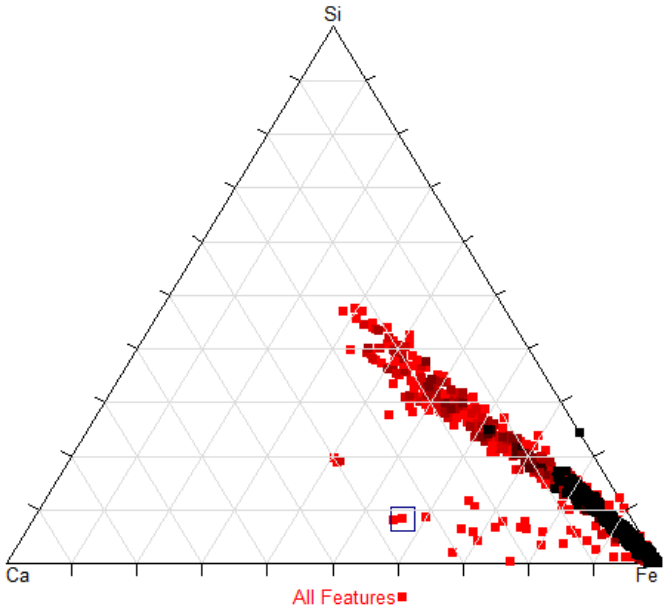

Figure Ternary plot of silicon, calcium and iron showing the main trend line running out from the iron-rich corner towards the Si-Ca side of the diagram. However a second less obvious trend line is present with a higher Ca to Si ratio (marked).

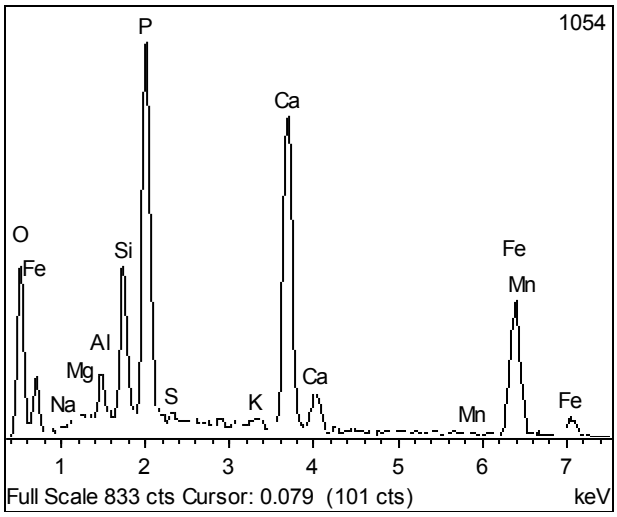

Figure Composition of marked inclusion showing very high phosphorus content.

Figure Plot of hardness verses distance for sample SF851

SF333 (Wedge type 1)

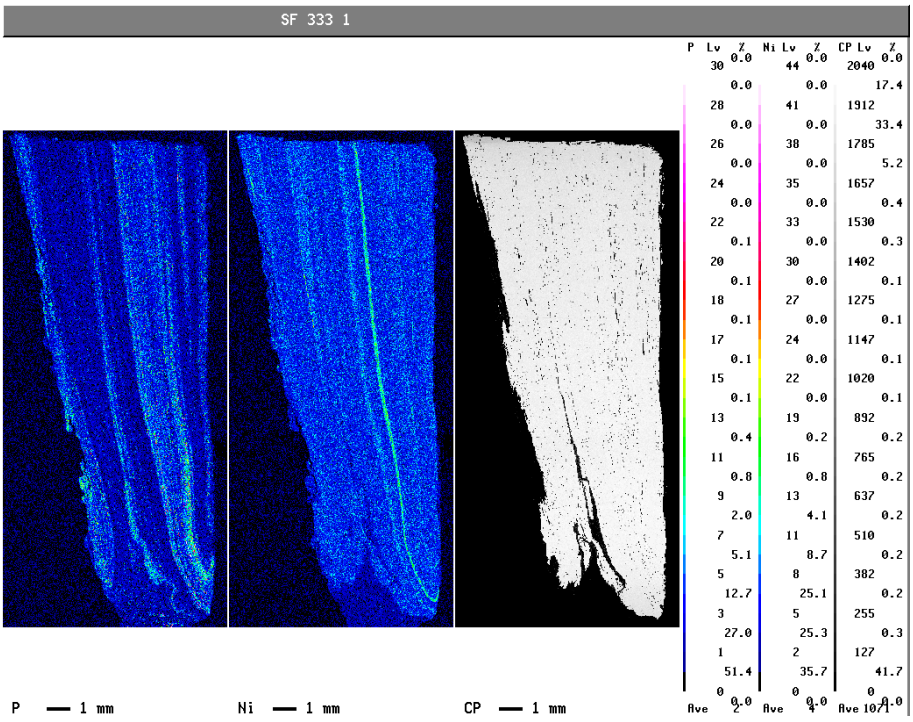

Figure Phosphorus, nickel X-ray maps and back-scattered electron image of Sample SF 333

The most obvious feature of this sample other than the pronounced cracking at the blade edge was the presence of a strong narrow bright line in the nickel X-ray map. Such lines are indicative of the location of a weld line. The whole structure is rather variable as can be seen by the variation in the grain size observed in Figure 31. The range of inclusions seen was similar to that in SF 851, that is, single phase, dual phase (iron oxide and 'glass' matrix) and some three phase inclusions. However, no distinct groups based on their composition could be determined by this initial analysis, although there was still some evidence of the separation a trend line of calcium and phosphorus inclusions (Figure 32). Also there were a few inclusions with sulphur contents greater than 4% weight.

The nickel content of the metal was, in general, around 0.02% although in some areas it fell below the detection limits of the EPMA. However, at the weld a nickel content of 0.44 % was measured.

The harness was relatively uniform across the sample, but without the usual increase in hardness towards the edges.

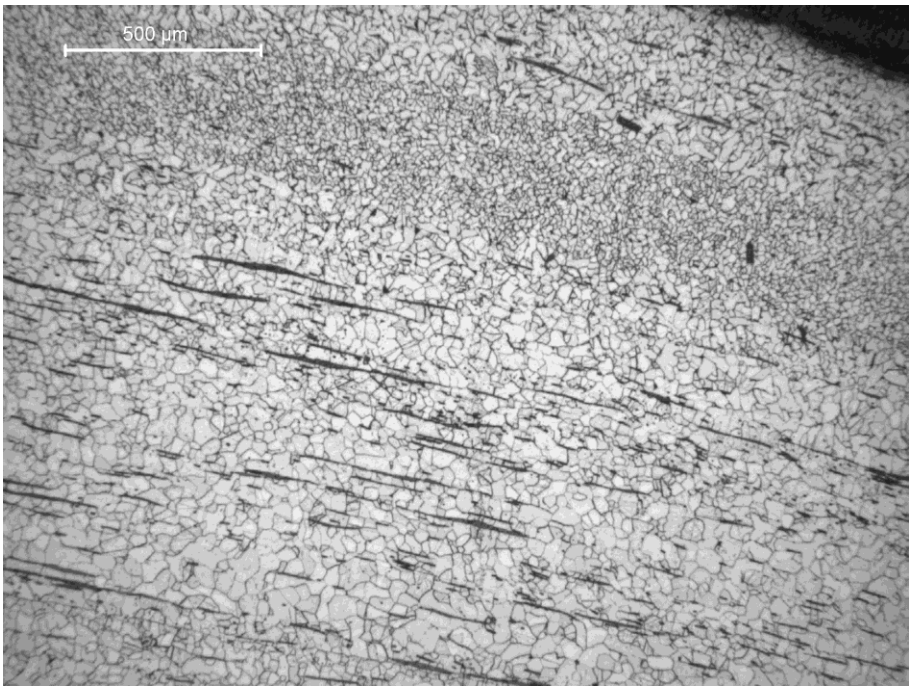

Figure Metallographic image showing the variable banded structure of sample SF 333

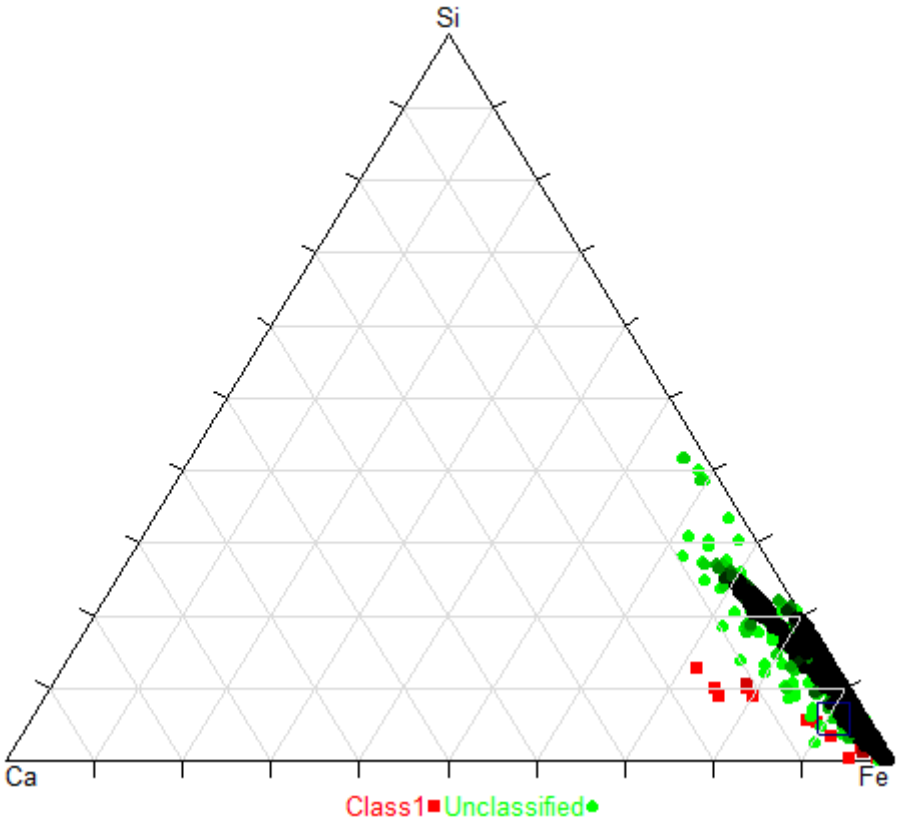

Figure Ternary plot of inclusions showing those inclusions with a high calcium to silicon ratio as Class 1

Figure Plot of hardness verse distance across sample SF 333

SF530 (Wedge type 3)

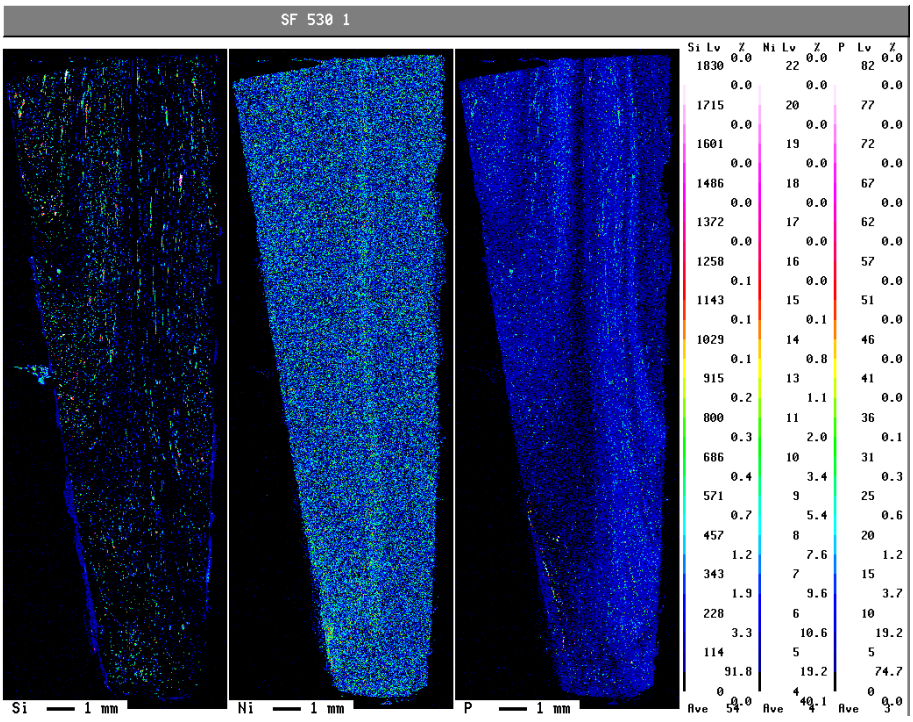

Figure Silicon, Nickel and phosphorus X-ray maps of Sample SF 530

The X-ray maps of Sample SF 530 suggest that the metal may have been welded together, as is indicated by the faint increase in nickel (Figure 34) which is partially mirrored by a narrow band with low phosphorus. However, the nickel line is not well defined unlike the one seen in sample SF 333. This probably means that either the weld was one that occurred during the primary manufacture of metal, or if the weld occurred during the manufacture of the wedge it has been subjected to prolonged periods at high temperatures, so that the nickel has time to diffuse away from the weld line. In addition, there is small region at the tip of the blade where there was a different piece of metal inserted. This is more easily seen in the silicon and sulphur X-ray maps (Figure 35) where there is a small triangular region with higher density of slag inclusions containing sulphur.

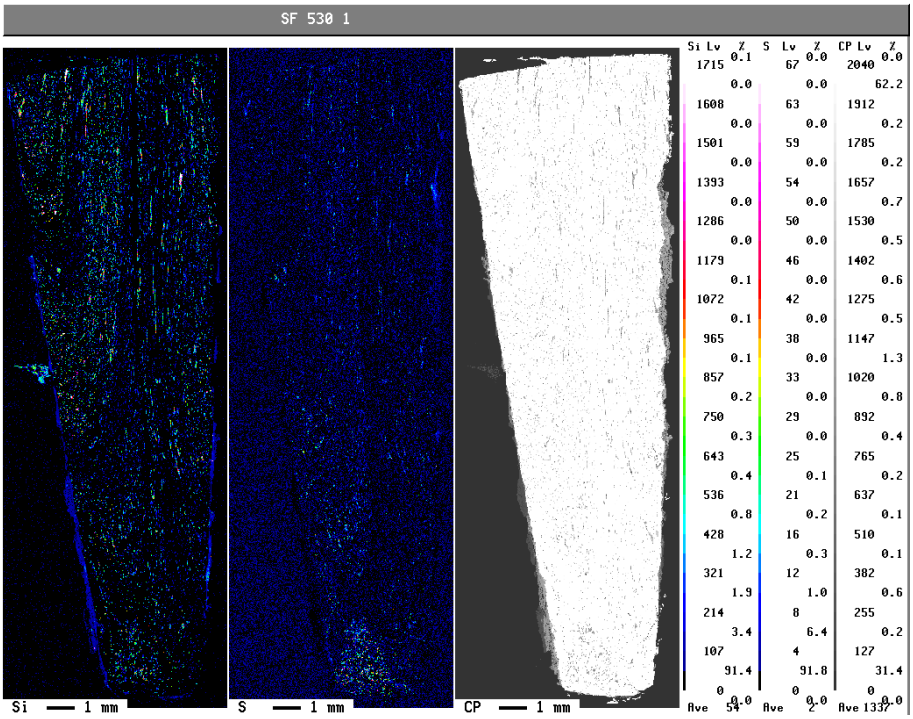

Figure Silicon, and sulphur X-ray maps and back-scattered electron image of Sample SF 530

The silicon image shows that the high slag density as does the metallographic image (Figure 36), which also shows the bands of large and small grains. The presence of such grains is typical of bands with low carbon and high phosphorus. In this case the sample had average phosphorus content close to 0.13% and the percentage area of the polished covered by slag inclusions was twice of the samples covered above. The inclusions tended to be of two forms. Either small rounded single phase inclusions of silicon-phosphorus-iron oxide with the proportion of silicon to phosphorus varying (Figure 37 Spectrum 1 where the phosphorus peak is much higher than the silicon), or more elongate multiphase inclusions (Fig 37 spectra 2 and 3) with a matrix of an iron-silicate with an appreciable amount of phosphorus, with small contributions from aluminium and sulphur, and iron oxide as the second phase. When other inclusions were examined at higher magnification it was clear that there was at least four phases present. They were iron oxide, an iron silicate with phosphorus growing as fine dendrites, a calcium rich matrix between the dendrites and small iron sulphide particles (Figure 38). Compositionally the inclusions could not be separated into groups. However, due to the method used to acquire compositional data the small round inclusions would not have been included in the analysis.

The high hardness is not unexpected with the levels of phosphorus seen in this material.

Figure Image of Sample SF 530 showing high density of slag inclusions and bands of small and large grains.

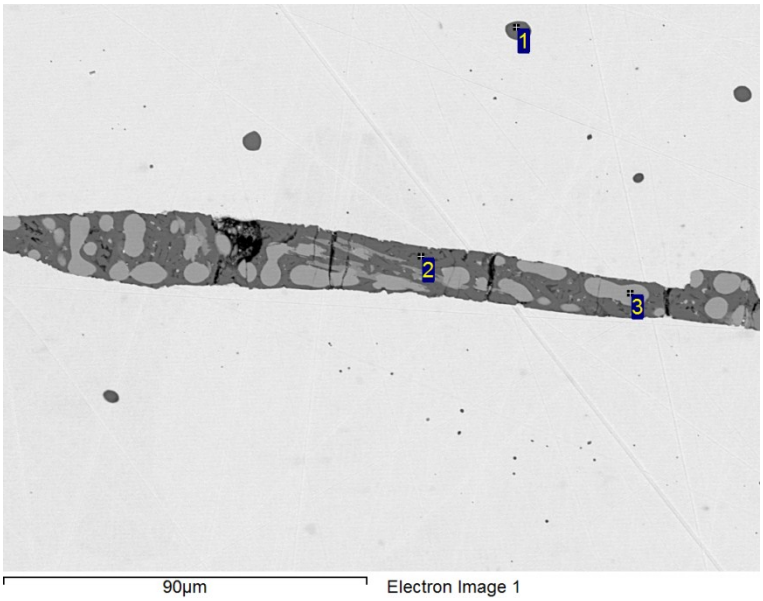

Figure Typical inclusions seen in SF530, small round single phase, or more elongate multi-phase

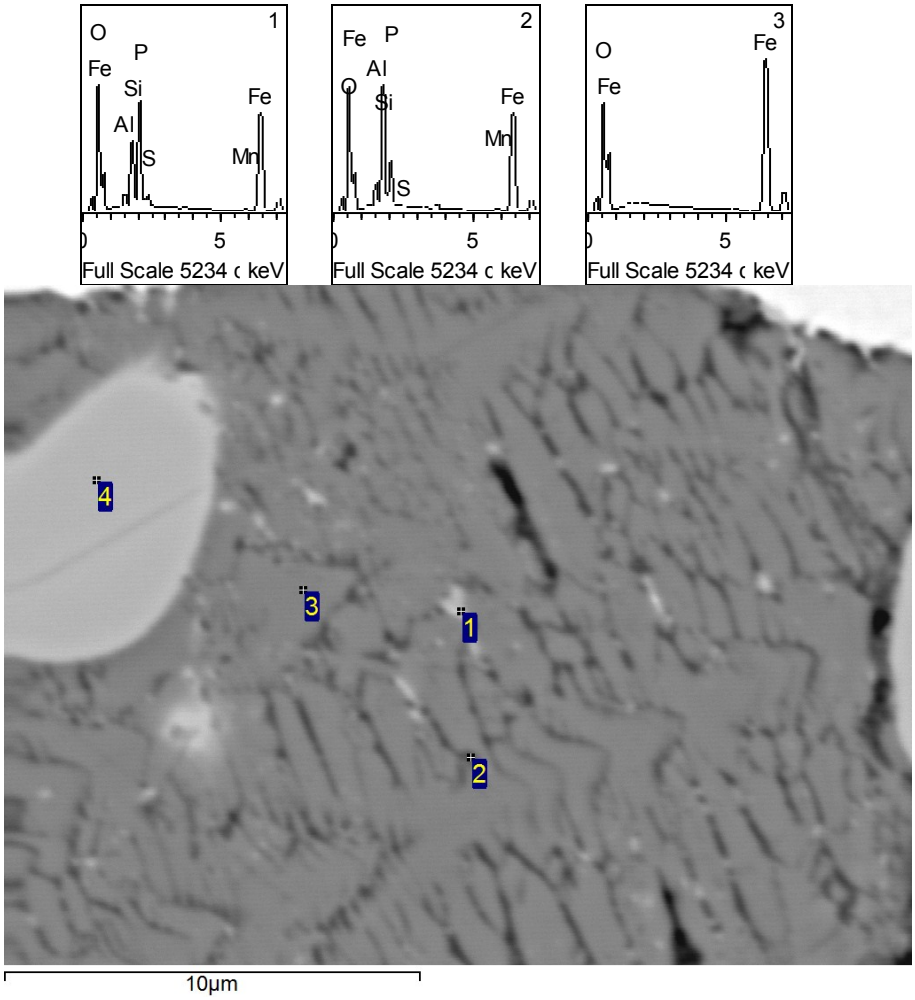

Figure Detailed view of multiphase inclusion showing rounded iron oxide(4), fine dendritic growth of iron silicate(3), in matrix containing calcium, and small bright particles of iron sulphide(1)

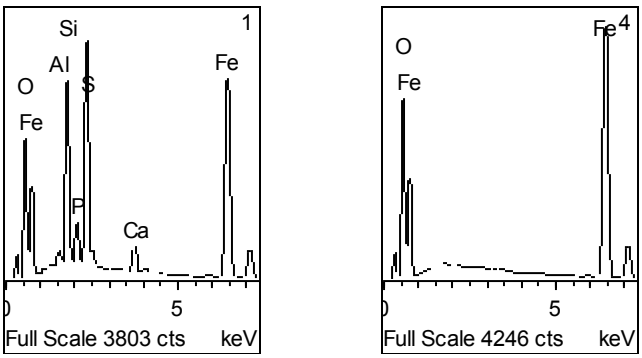

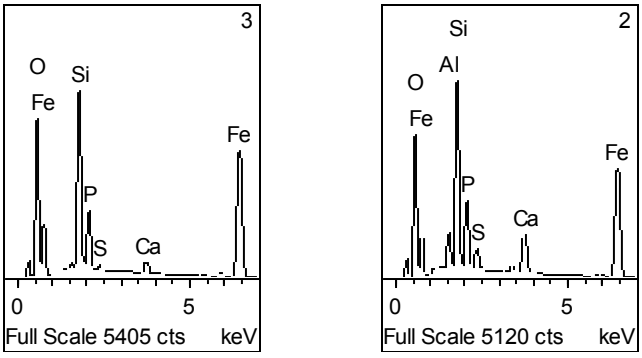

Figure Plot of hardness against distance for sample SF 530

SF373 (Wedge type 3)

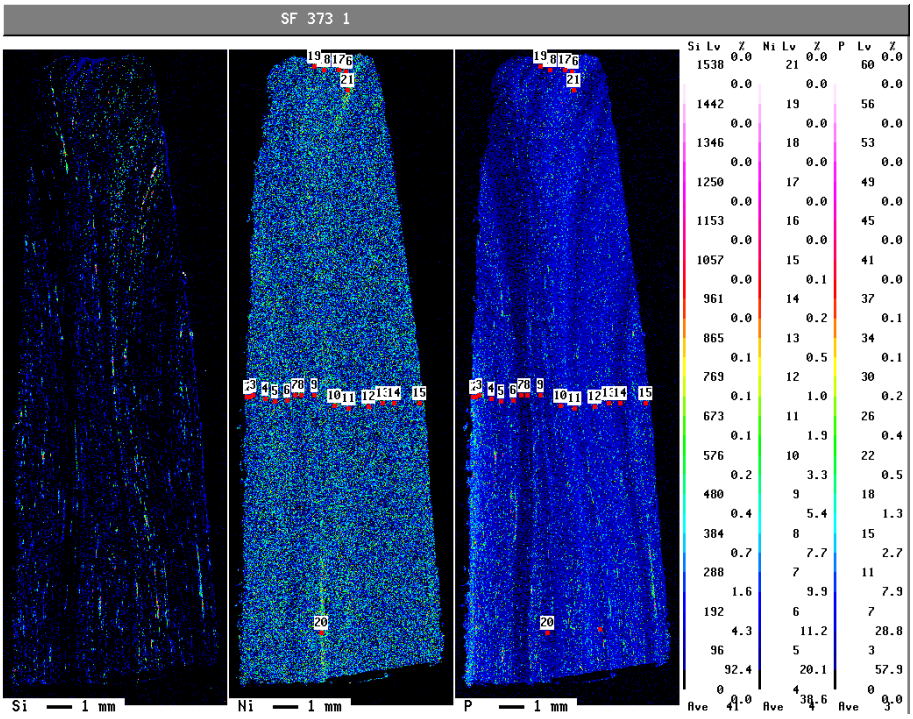

Figure Silicon, Nickel and Phosphorus maps for Sample SF 373

In most ways this sample was very similar to SF 530 with a high density of slag inclusions, and similar high phosphorus content and it was not possible to separate the inclusions any composition groups. The microstructure of the metal was slightly less banded in terms of grain size as is shown by Figure 41. There appeared to be more multiphase inclusions than in sample SF 530, the phase morphology of some of those inclusions was more complex. There were the standard two phase iron oxide and iron-silicon-phosphorus oxide inclusions, in which the iron oxide was in rounded form, but in addition there were inclusion in which a phase rich in iron oxide grew in a lathe form (Figure 42, 3). This iron oxide phase is different from the rounded form that is also present in the inclusion (42.1) in that its back-scattered signal in darker than the rounded form (FeO) and it contains a few percent of silicon and phosphorus and a trace of aluminium. These inclusions also contain iron sulphide inclusions (42.4). In some case the iron oxide content of the slag inclusions was very high (Figure 43) so that the two forms of the iron oxide occupied most of the cross-section and there was only a little of iron-silicon-phosphorus matrix present. In the case of the inclusion in Figure 43 there was still iron sulphide present as can be seen by the numerous small bright particles within the inclusion.

The hardness of this sample was lower than sample SF 530. The hardness did rise at the edges. This could have been partially due to some work-hardening, but it also reflects changes in the phosphorus content of the metal and minor changes in the carbon content. The higher hardness did tend to occur in regions with phosphorus ghosting present.

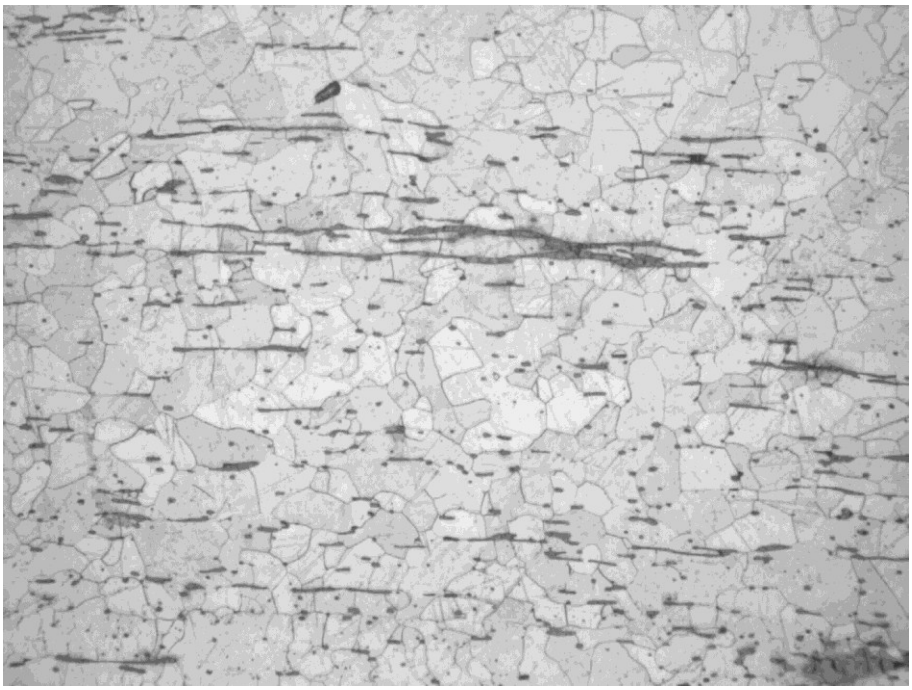

Figure Metallographic image of sample SF 373

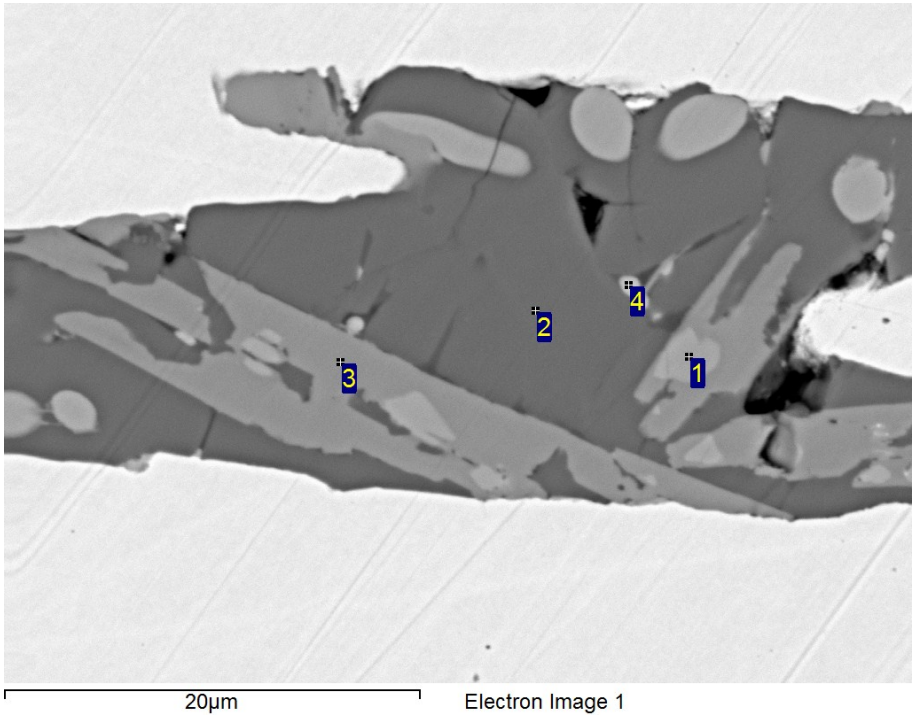

Figure Inclusion showing lathe morphology phase (spectra shown below)

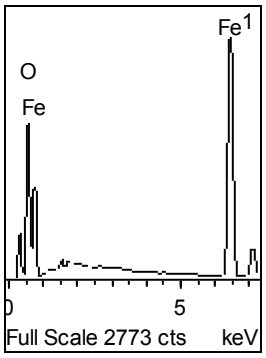

Iron Oxide

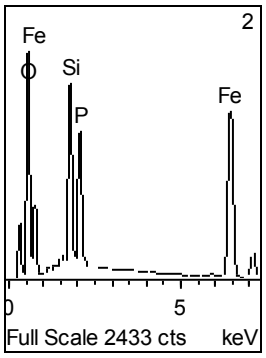

Main matrix Fe-Si-P oxide

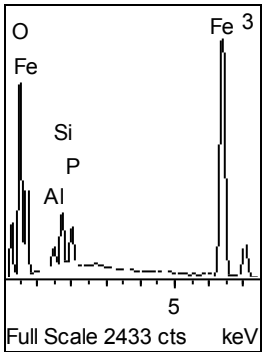

Iron Oxide with Si, and P

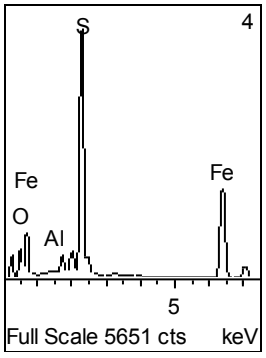

Iron Sulphide

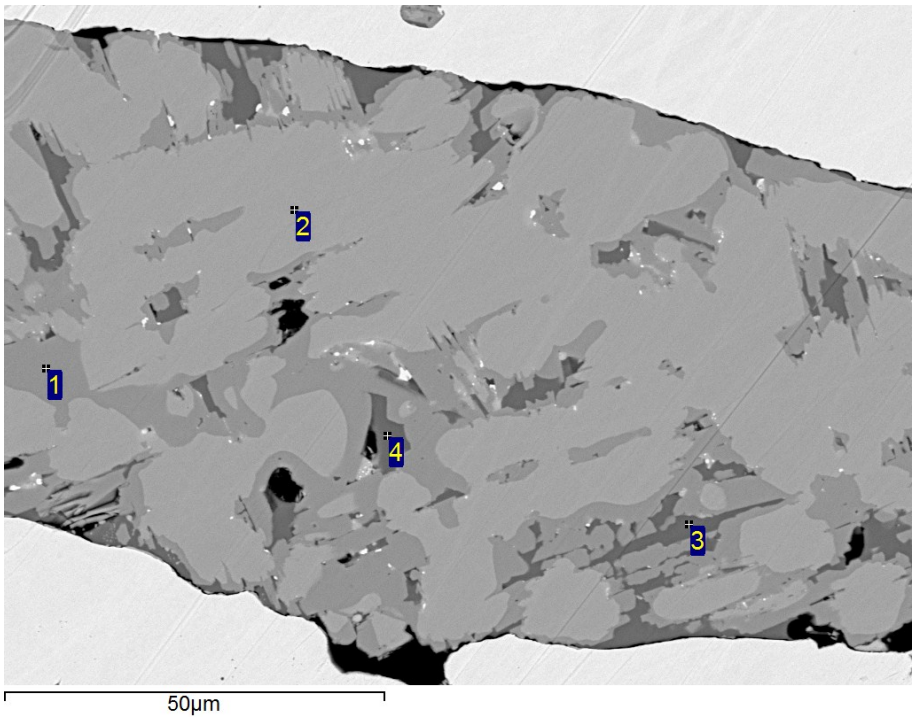

Figure Back-scattered electron image of slag inclusion with high iron oxide content.

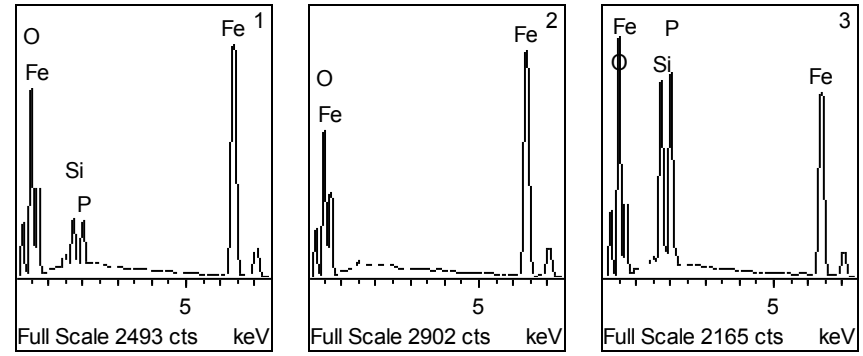

Iron Oxide with Si and P Iron oxide Normal matrix phase

Figure Plot of hardness against distance in mm.

SF623 (Wedge type 2)

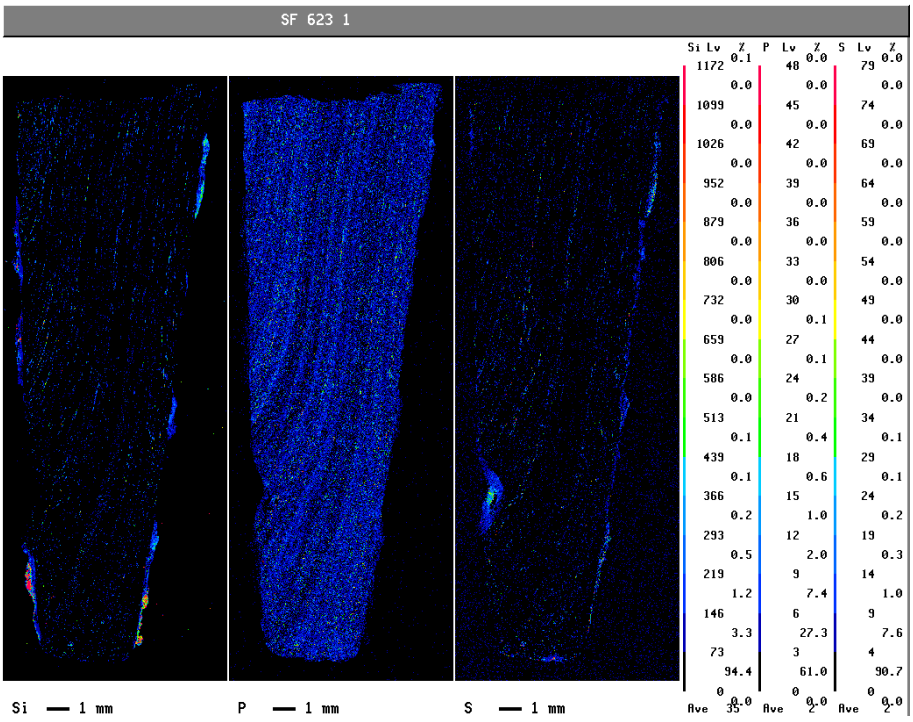

Figure Image showing the silicon, phosphorus and sulphur X-ray maps for sample SF 623

The X-ray maps show the usual parallel banded structure of varying phosphorus contents. Although the overall phosphorus content of this sample was lower than the rest of the late period wedges (SF 530, 373, 623 and 1030) it varied between 0.02 % in one of the low bands to a maximum of 0.14 %. The grain size was as usual variable but was the sample with the largest grains (smallest grain size number). It was also one of the softer samples which might be expected given this combination of grain size and phosphorus content. The hardness does increase towards the edges which is no doubt due to a combination of the distribution of phosphorus and the mechanical history of the blade.

The inclusions were similar to those found in sample SF 373, in that they contained two type of iron oxide, the normal version with only iron and oxygen, and type with an appreciable quantity of silicon and phosphorus, both in a matrix of iron-silicon-phosphorus oxide (Figure 47). Like samples SF 373 and SF 530 in did not prove possible to discriminate any inclusion composition groups.

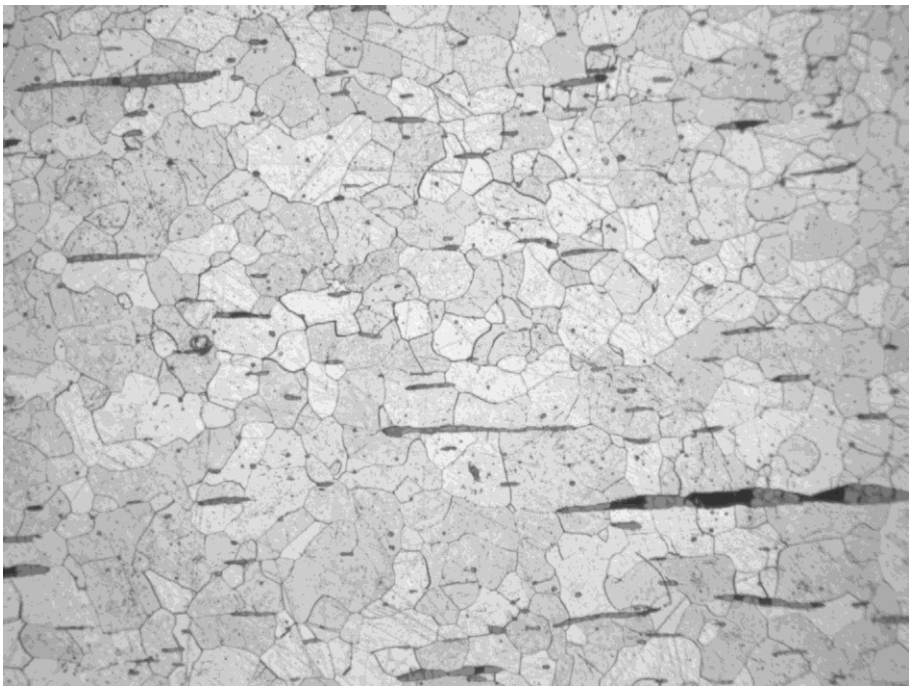

Figure Metallographic image of sample SF 623

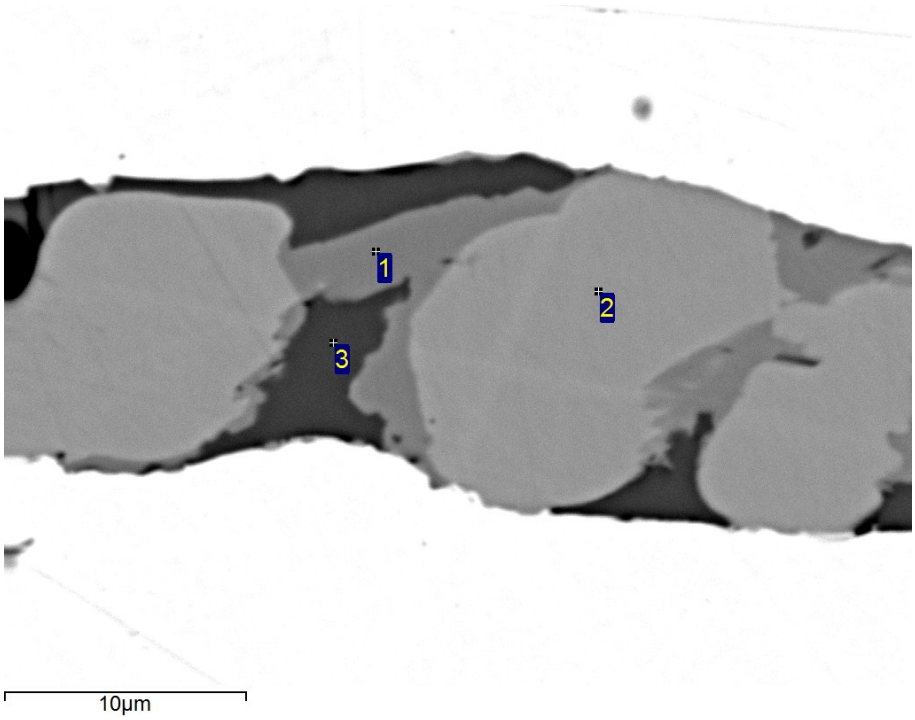

Figure Back-scattered electron image of a multi-phase slag inclusion from sample SF 623, spectra given below.

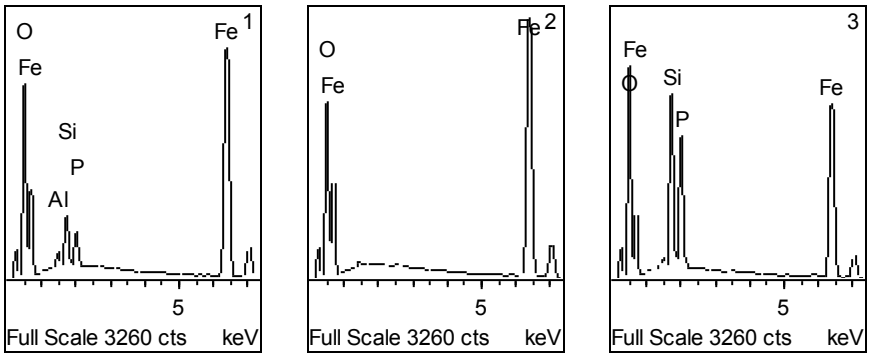

SF1030 (Wedge type 2)

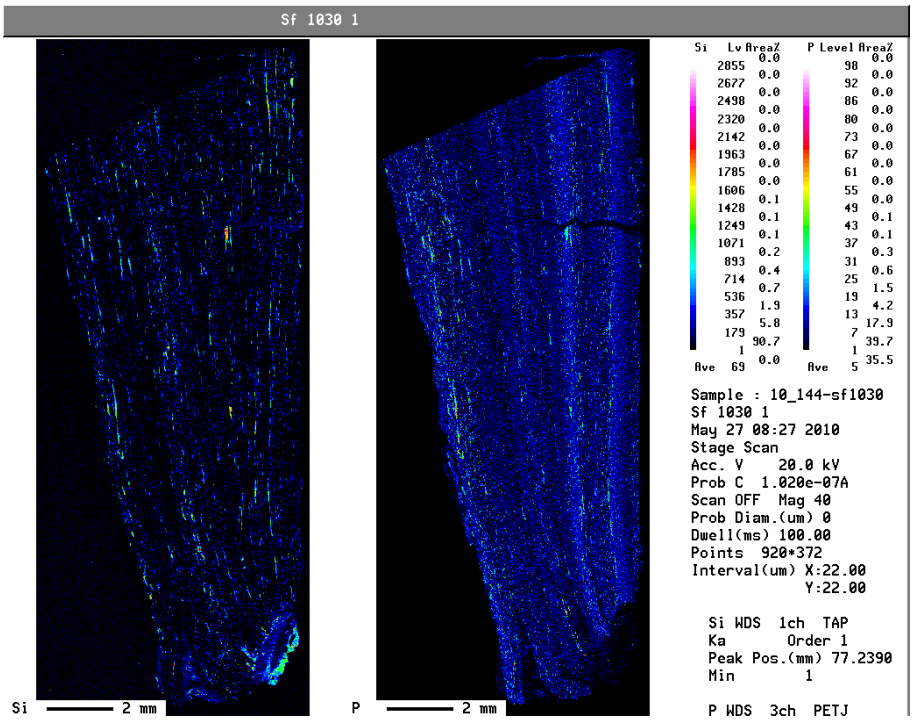

Figure Silicon and phosphorus X-ray maps of sample SF 1030

This sample shows the usual phosphorus banding, but also there is considerable delamination along the forging plane at the blade and a transverse crack further up the sample. The transverse crack (visible in phosphorus map in Figure 48, and the back-scattered electron image Fig 49) is almost certainly the result of mechanical misuse. This wedge was severely bent suggesting that it had either been used as a lever, or has become stuck and it was attempted to lever the wedge out. Although the presence of phosphorus increases the hardness of iron, and thus improves its wear resistance, it also reduces its ductility at ambient temperatures making more susceptible to cracking. The very high density of slag inclusions (Figure 50) would further increase the likelihood of crack to occur.

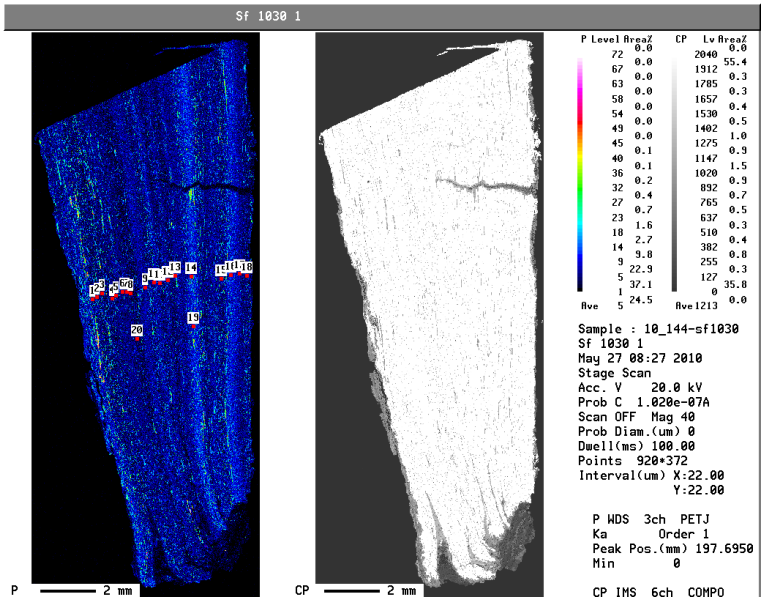

Figure Phosphorus and back-scattered electron images

The presence of a high phosphorus bands can be seen running across the centre of Figure 51 by the presence of zone of grains with an internal ripple-like structure. This is a case of heavy phosphorus ghosting.

Figure 52 shows one of the fields randomly selected to characterize the types of inclusions present. In this image it can be seen that the majority of the inclusions are multi-phase. However, one dark inclusion is single phase with a calcium-phosphorus iron oxide composition. The other inclusions have a silicon-phosphorus-iron oxide composition with a little alumina and sometimes traces of calcium. Figure 53 shows a plot of calcium against silicon for the approximately 4700 inclusions in the database for this sample. Only 4 had compositions similar to the dark inclusion (Class 1). This plot showed that it was possible to determine two compositional trend lines for this sample based on the ratio of calcium to silicon. The class 3 inclusions had some calcium where the class 2 inclusions had only very low levels of calcium. The morphological difference between these two types of slag appears to be that the class 2 inclusions are single phase (Figure 54.1). In the region of Figure 54 all the class 2 inclusions were small and round but in other regions they did take on elongate forms. One of the unusual feature of the slag inclusions in this sample compared with all the other wrought iron samples was the ubiquitous present of a few percent of manganese. Figure 55 shows that the manganese occurs in greater concentrations in the matrix phases rather than the iron-oxide phases. The rounded form of iron oxide (55.1) contained traces of titanium and vanadium as well as manganese whereas titanium and vanadium was not seen in the lathe form of the iron oxide (55.2). Many of the inclusions in sample SF 530 had appreciable manganese content but it was not nearly every inclusion as seen in SF 1030.

The hardness is consistent with the phosphorus content (varying between 011 and 0.33 %) although the rise in hardness at the start of the hardness trace (Figure 56) is not explained by a corresponding increase in phosphorus content. This is additional hardness is likely to be due to mechanical mistreatment that this sample suffered.

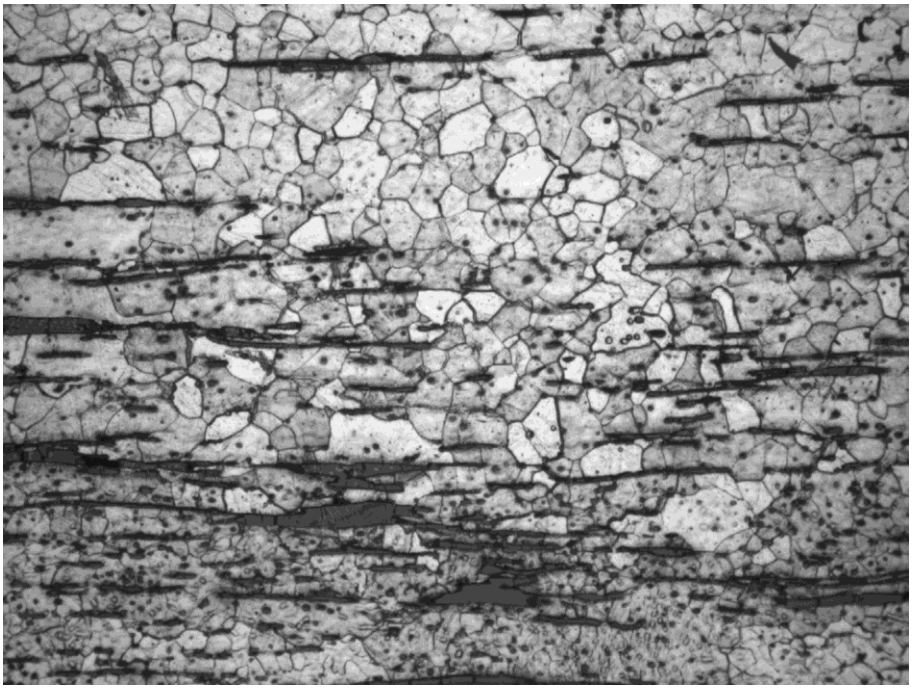

Figure Metallographic image of SF 1030 showing high density of slag inclusions.

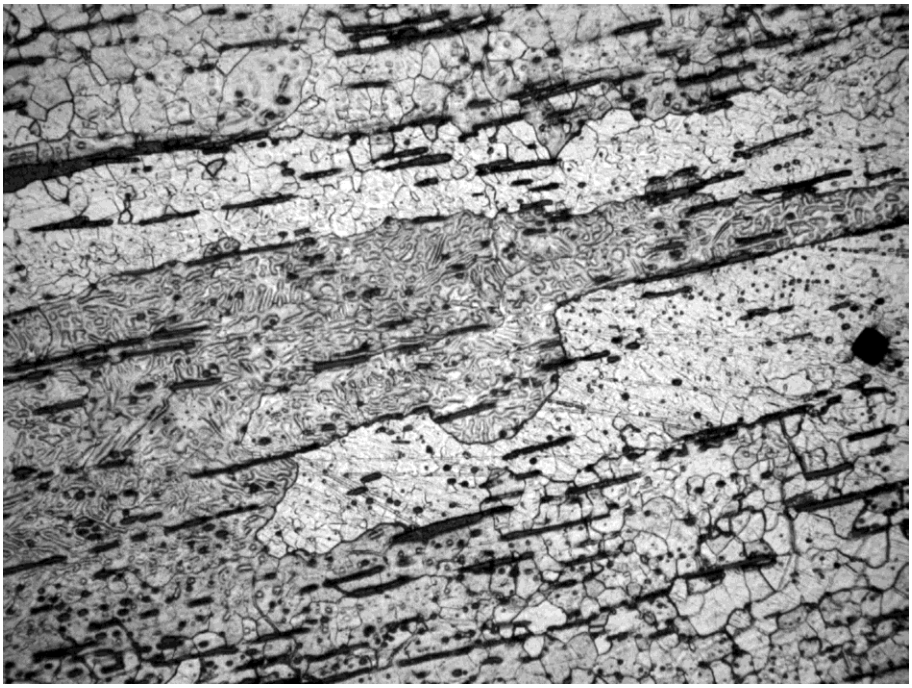

Figure Metallographic image of SF 1030 showing an area of large grains with strong phosphorus ghosting.

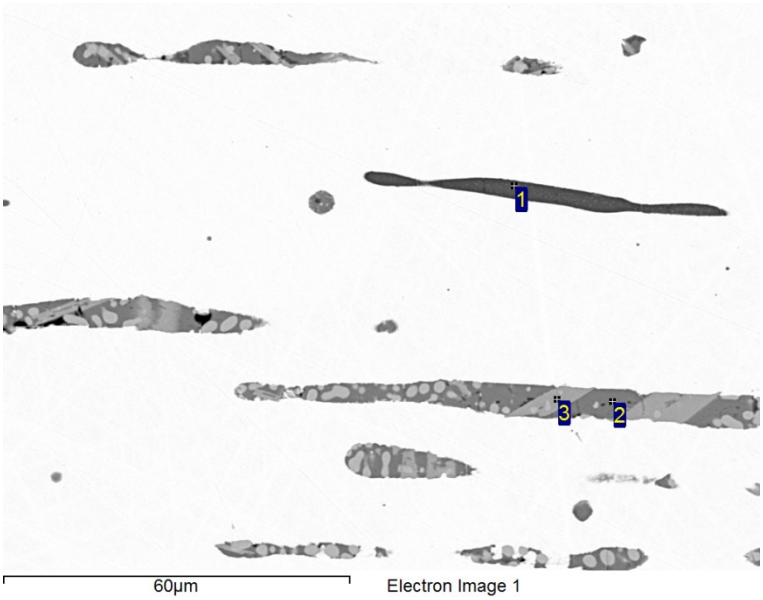

Figure Back-scattered electron image of an unusual dark inclusion (1) and normal multi-phase inclusions.

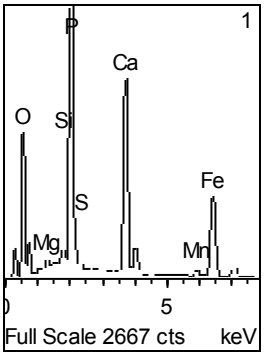

Dark inclusion

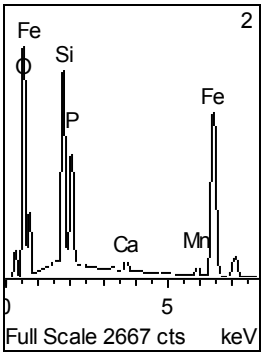

Normal matrix

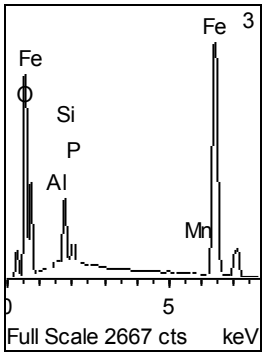

Lathe Si-P iron oxide

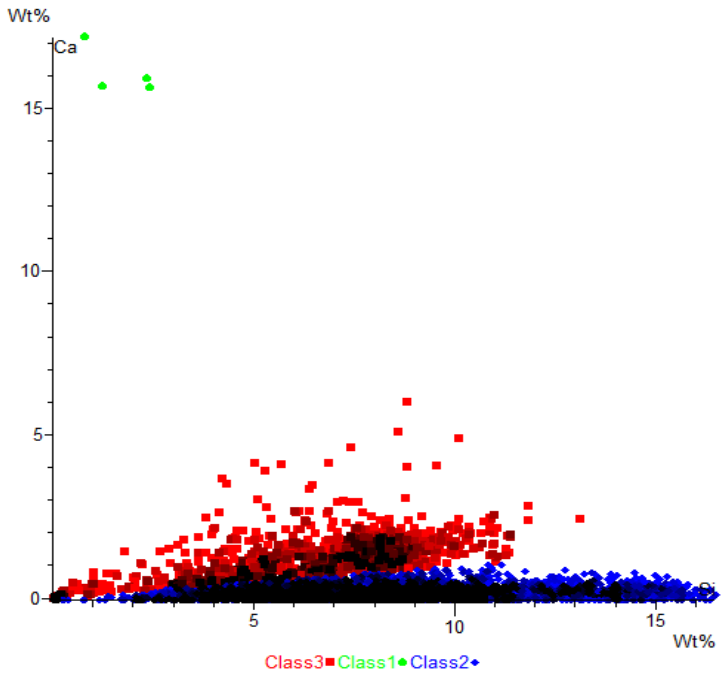

Figure Inclusion composition grouping

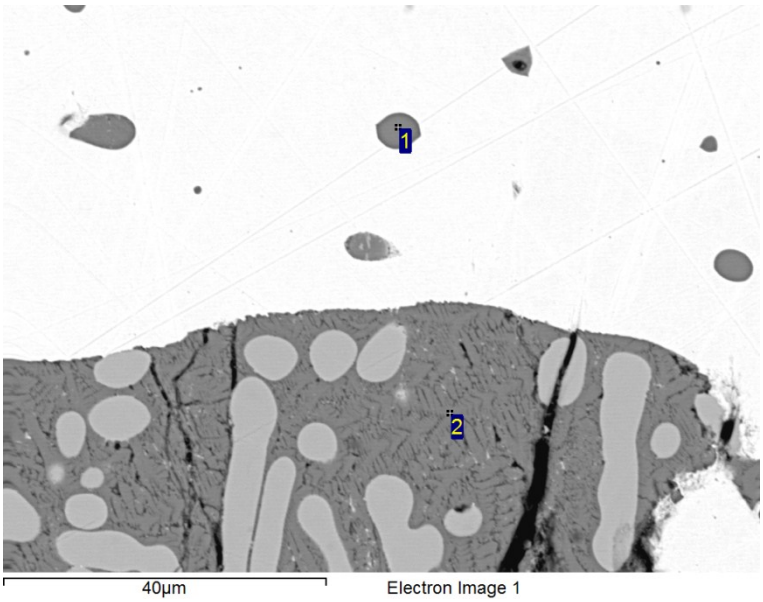

Figure Back-scattered electron image of single phase inclusion showing inclusions with low calcium (1) and multiphase inclusion (2) with calcium. The spectra are given below.

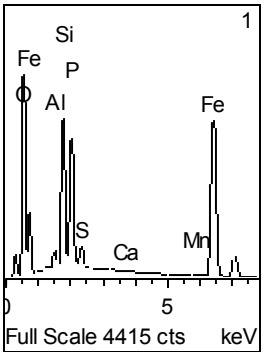
1
Si
Fe
P
O
Al
Fe
S
Ca
Mn
0
5
Full Scale 4415 cts
keV

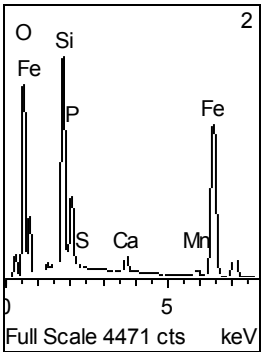
2
O
Si
Fe
P
Fe
S
Ca
Mn
0
5
Full Scale 4471 cts
keV

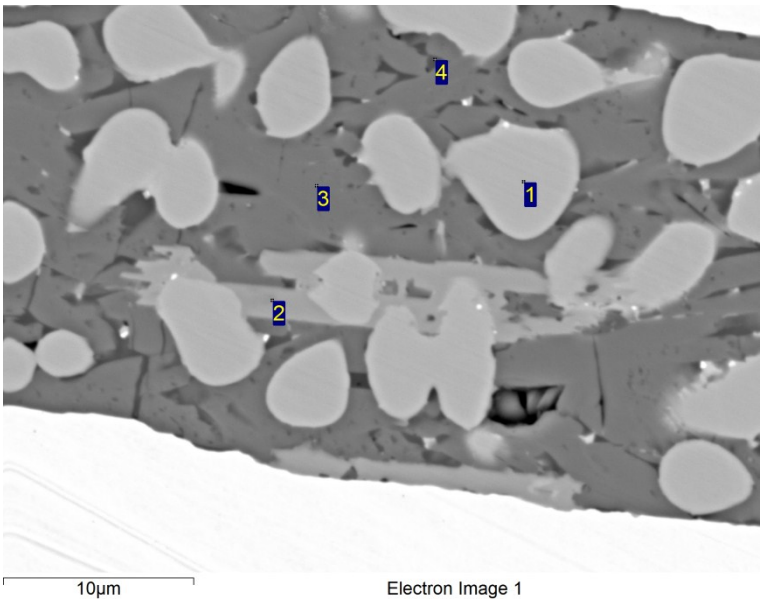

Figure Detailed view of a multi phase inclusion showing bright sulphides as well as the phases indicated by the spectra below

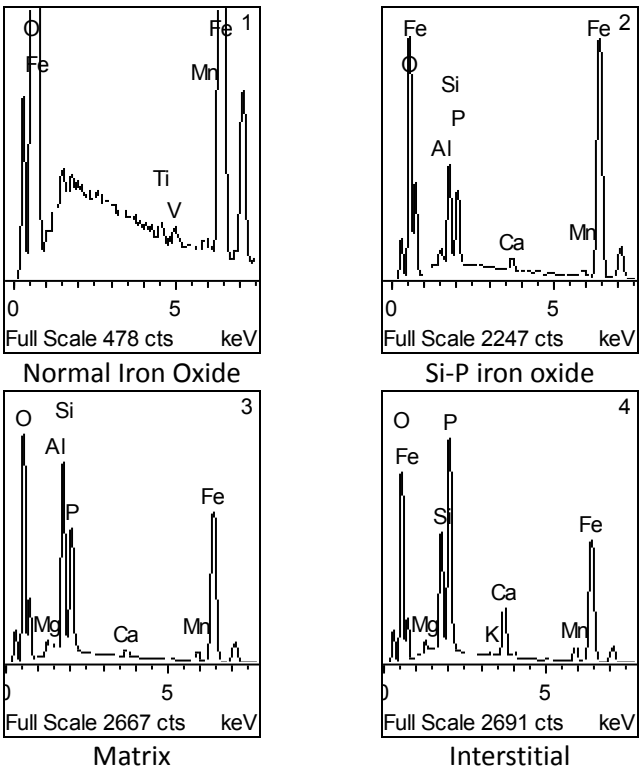

Figure Plot of hardness against distance in mm.

Discussion

Given the late 17th or early 18th century date given to the saw (SF 632) a study of its composition and microstructure would have been extremely interesting as there have been very few studies of steel from this period. However, the uniform hyper-eutectoid composition and the presence of both silicon in the metal and of manganese-iron sulphide inclusions indicate that it is not consistent with the methods used to produce iron (the charcoal blast furnace and the finery) and then to convert this iron to steel by carburization. It was more likely to have been produced by a liquid steel-making process after the introduction of coke-fired blast furnace, after 1709 at the earliest. But as the iron from the early coke-blast furnace was not considered suitable for steel making this item is likely to date from much later. The fact that there was a high proportion of silicate and other non-sulphide inclusions present and that there was not enough manganese to entirely prevent the formation of iron sulphide would suggest a late 19th century date for this sample.

The saw was the only artefact made of steel studied; all the wedges were of phosphoritic wrought iron without any attempt to harden the faces or 'cutting' edge by carburizing. The use of phosphoritic iron would have made an attempt to do so difficult, as phosphorus slows the diffusion of carbon into iron. In most cases, the hardness of the combination of phosphorus content and work-hardening have improved the properties considerable above those that would be obtained from a plain wrought iron. Only sample SF 851 from phase 2 had the sort of hardness that might be expected from a non-phosphoritic iron although it did have an appreciable phosphor content. The cause for this discrepancy is not obvious and would require further investigation.

A number of the samples showed one of the problems with the very directional nature of wrought iron, which is cracks and corrosion running along the planes of high slag inclusion density. Mostly this was in the form of cracks running back from the blade. This was seen in samples SF 333 and SF 1030, however, sample SF 1030 suffered transverse cracking and subsequent corrosion along the slag inclusions exposed. In the case of ST 1030 the transverse cracking is likely to be a result of the heavy mechanical misuse that this sample has suffered. It had been bent in the plane of the wedge, no doubt due to the wedge having been used as a lever rather than a wedge.

Killick and Gordon (1987) in their study of puddling slags noted that puddling slag was poor in the alkali element and in potassium in particular. The main source of potassium would have been the charcoal fuel ash, which would not get into the slag as the fire and the working area in the puddling furnace were separate. Examination of table 4 shows that samples SF 917 and SF 851, from phases 1 and 2, have a noticeably higher potassium contents than the wedges from most of the later wedges (SF 530, 373, 623 and SF 1030). This is entirely consistent with the history the transition from the finery to the puddling furnace, in that the finery was the main method of producing wrought iron from cast iron until the 1770s. Sample SF 333 form either phase 3 or 4 had an average potassium slag inclusion composition intermediate between that of samples SF 917and SF 851, and the rest of the later material. The slag inclusions also had a lower average phosphorus content similar to the two earlier samples. This might be simply due to pig iron used having a lower phosphorus content or

could be a result of process being used. As such it not clear whether this sample should be ascribed to the finery process or an early version of the puddling process which used fluxes other than silica or iron oxide. The later wrought iron all had high phosphorus contents and the matrix of the slag inclusions was either iron-phosphorus silicate, or the unusual iron oxide formed a considerable proportion of the inclusion area. Whereas, the inclusions form the earlier samples had either a high silica glass matrix or fayalite had crystallized. However, Mackenzie (2006, 144, 145) studying 19th century raw material for the blister steel industry reported that the inclusions had a 'fayalitic' matrix with wüstite (FeO) dendrites but there was no mention of the other elements. Therefore one could assume that they were not present in significant quantities.

The sulphur content did not distinguish any of the samples other than the steel, therefore it is likely that all the pig iron used was smelting in coke fired furnaces rather than charcoal-fired furnaces. Although, it is not possible to provenance wrought iron on such a small element set, it is possible to conclude that the ore that was smelted to produce pig iron came from source with high phosphorus content. This would rule out the low phosphorus ore of the Forest of Dean. It is more likely that ores associated with the coal fields were the source of pig iron where the nodular ore often have high level s of phosphorus.

Given the size of the sample it is difficult to determine if a phosphoritic iron had been deliberately selected for the manufacture of these wedges, or it was used because it was the cheapest local supply to the manufacturer. The use of phosphoritc iron would have certain mechanical advantages as long as the wedges were used in the manner intended (in compression).

Conclusions

It is likely that the saw, SF 632 does not belong to phase 1 due to its high density of MnS/FeS/FeO inclusions. Such as steel is more likely to belong to the late 19th or early 20th century.

It is possible determine that SF917 and SF851 were made from finery iron rather than puddle iron on the basis of their potassium contents.

Given the high sulphur content of the slag inclusions it is likely all the pig iron was produced in coke-fired blast furnaces.

The later wedges (SF 530, 373, 623 and 1030) are all consistent with having been produced using the puddling furnace, however, SF 333 shows a number of characteristics intermediate between the finery and puddled iron.

The chance location of the high calcium phosphorus inclusions in the first standard SEM field of view of sample SF 1030 shows the dangers of only analyzing a small number of inclusions which has been the normal practice. These inclusions only occurred at a rate of 1 in 1000 over the large scan, whereas it was one of ten in that field of view.

In samples it is possible to form compositional groups based on the relative proportion of the elements present. The further study of these groups and the reasons for their formation should reveal information about the processes involved the production of the finished metal.

This group of tools (wedges) was made consistently of high phosphorus iron rather than steel. Further work needs to be carried out to determine if this is just a local phenomenon, or is the case country-wide. Also, it would be interesting to determine when such tools began to be made of steel rather than iron.

References

Cleere, H. and Crossley, D., 1985, *The Iron Industry of the Weald*, Leicester University Press,

Blakelock, E., Martinón-Torres, M., and Young, T., 2009. Slag inclusions and the quest for provenance: analysis of slag and slag inclusions from iron smelting experiments. *Abstracts of the World of Iron Conference*, London. 52-53

Day, J., and Tylecote, R.F., 1991. *The industrial Revolution in metals*. The Institute of Metals, London.

Dillmann, Ph., l'Héritier, M., LeFebrvre, E., and Timbert, A. 2009, 'From Soissons to Beauvias: Ferrous reinforcements in Gothic cathedrals from Picardy', *Abstracts of the World of Iron Conference*, 48, London.

Ehrenreich, R.M. 1985. '*Trade, Technology and the iron working community in the Iron Age of Southern Britain*', BAR British Series 144, Oxford

Hayman, R. 2004, 'The Cranage Brothers and eighteenth century forge technology', *Historical Metallurgy*, **38 (2)** 113-120.

Killick., D. and Gordon, R.B. 1987. 'Microstructures of puddling slags from Fontley, England and Roxbury, Connecticut, USA.' Journal of the Historical Metallurgy Society 21(1) 28-36

Mackenzie, R.J. and Whiteman, J.A., 2006, 'Why pay more? An archaeometallurgical investigation of 19th century Swedish wrought iron and Sheffield blister steel', *Historical Metallurgy* **40(2)** 138-149.

Mertens, A., Mathis, F., Dillman, Ph., and Hoffsummer, P. 2009. Iron production in the region of Liège in the Middle Age: Contribution of slag inclusions analyses performed on ferrous reinforcements from medieval frames data by dendrochronology, *Abstracts of the World of Iron Conference*, 48-49 London.

Rostoker W, and Dvorak J. 1988. 'Blister steel = Clean Steel', *Archaeomaterials* 4, 175-186

Rostoker W, and Dvorak J. 1990. 'Wrought irons: Distinguishing between processes', *Archaeomaterials* **4**, 153-166

Tylecote, R.F. 1976. *A History of Metallurgy*. The Metals Society. London.

Appendixes

EPMA analysis Conditions

SEM Analysis Conditions

Etching

Phosphorus ghosting

Hardness test